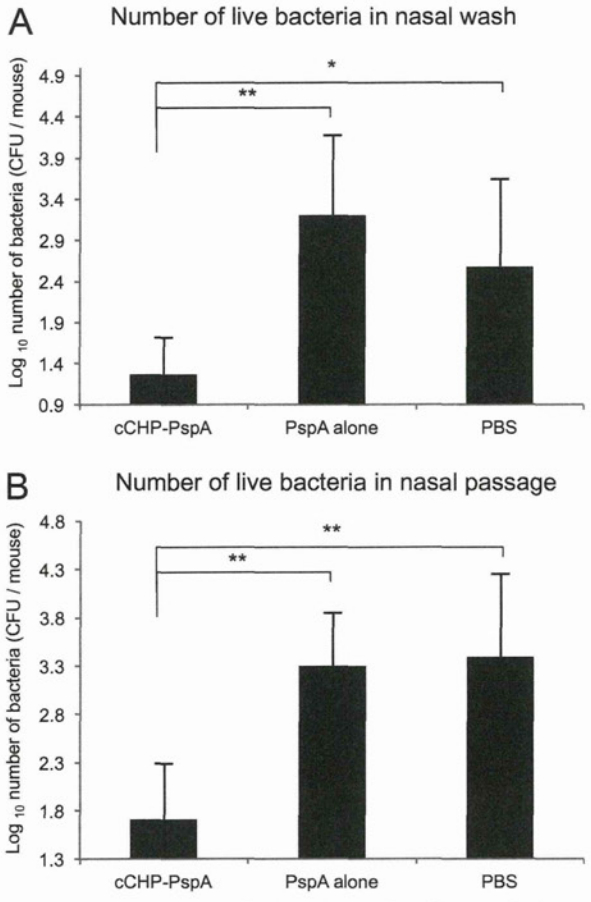

FIG 3 Intranasal vaccination with cCHP-PspA reduced bacterial colonization of the nasal cavity. One week after the final immunization, mice were challenged with a sublethal dose (2×10^4 CFU/mouse) of *Streptococcus pneumoniae* Xen10. Nasal washes and tissues were collected, and the numbers of *S. pneumoniae* Xen10 3 days after infection were determined. Data are representative of three independent experiments, and each group consisted of 5 mice. *, $P < 0.05$; **, $P < 0.01$. Abbreviations: cCHP, cationic cholesteryl group-bearing pullulan; PspA, pneumococcal surface protein A.

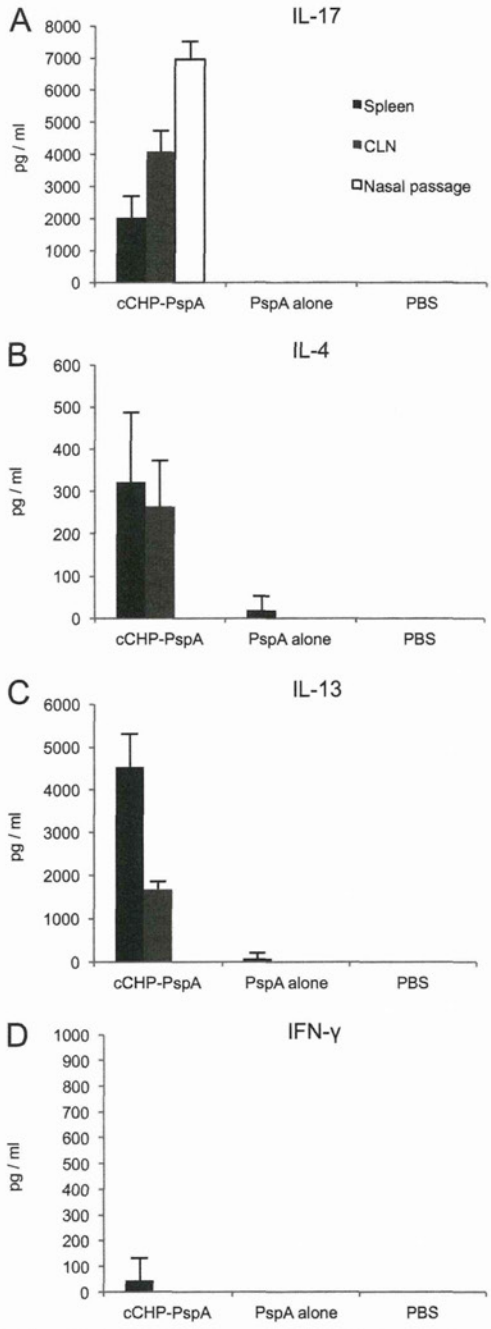

FIG 4 $CD4^+$ T cells from cCHP-PspA-immunized mice produce Th17- and Th2-type immune responses. Cytokines produced by $CD4^+$ T cells isolated from the spleens, cervical lymph nodes, and nasal passages of mice immunized with cCHP-PspA, PspA alone, or PBS only were analyzed. Data are representative of five independent experiments, and each group consisted of 5 mice. Abbreviations: cCHP, cationic cholesteryl-group-bearing pullulan; CLN, cervical lymph node; IFN-γ, gamma interferon; IL, interleukin; PspA, pneumococcal surface protein A.

PspA-specific mucosal IgA antibodies in the nasal secretions (Fig. 6A). In addition, BALF samples from mice intranasally vaccinated with cCHP-PspA contained PspA-specific IgA antibodies (Fig. 6B), and PspA-specific IgG antibodies were detected at high titers in both the NWs and BALF of mice intranasally immunized with cCHP-PspA (Fig. 6C and D). The nasal and BALF antigen-specific IgGs induced by intranasal immunization with cCHP-PspA were primarily of the IgG1 and IgG2b subclasses (Fig. 6E and F), similar to the Ig responses in the systemic compartment (Fig. 5B). Taken together, these results further support the benefit of cCHP-based nanogel as an effective nasal vaccine delivery vehicle for the induction of PspA-specific systemic and mucosal antibody responses against *S. pneumoniae*.

cCHP delivers PspA to dendritic cells (DCs) without CNS accumulation of PspA. The potential for antigen deposition and accumulation in the CNS through the olfactory fossa is one of the great concerns surrounding the use of nasal vaccines (33, 34, 50). To address this important concern, we instilled ^{111}In-labeled PspA alone or in complex with cCHP into the nasal cavities of mice. Beginning 6 h after administration, the nasal passages of mice treated with ^{111}In-labeled cCHP-PspA had higher SUVs than did those of mice treated with ^{111}In-labeled PspA alone, but there was no accumulation of ^{111}In-labeled PspA in the olfactory bulbs or brain throughout the 48-h observation period (Fig. 7A).

The cCHP vaccine delivery system enabled prolonged antigen exposure at the nasal epithelium, allowing continuous antigen

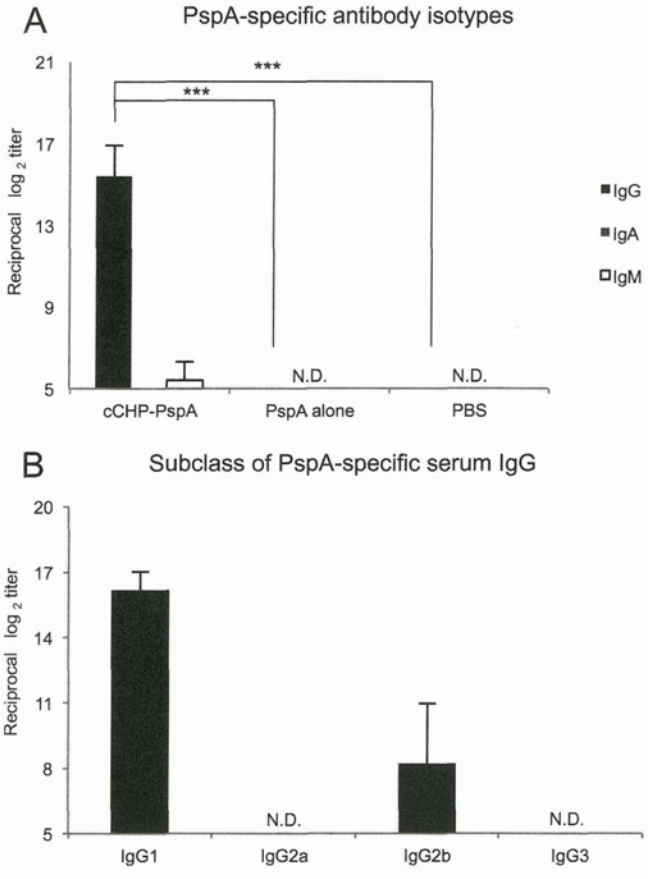

FIG 5 Intranasal vaccination with cCHP-PspA induced high levels of systemic antibodies. The data show the PspA-specific serum IgG level (A) and subclass analysis for IgG1, IgG2a, IgG2b, and IgG3 (B) for each immunized group (cCHP-PspA, PspA alone, or PBS only). Titers of PspA-specific IgG in sera were measured on day 7 after final immunization. Data are representative of three independent experiments, and each group consisted of 5 mice. N.D., not detected by ELISA with samples diluted 1:32. ***, $P < 0.001$. Abbreviations: cCHP, cationic cholesteryl group-bearing pullulan; Ig, immunoglobulin; PspA, pneumococcal surface protein A.

uptake by nasal DCs located in the epithelial layer and lamina propria of the nasal passages for the initiation of antigen-specific immune responses. Whereas 17.8% of the DCs located in the nasal passages had taken up PspA in the mice intranasally immunized with cCHP-PspA, only 0.7% of nasal DCs contained PspA antigen in mice that had been immunized intranasally with PspA alone (Fig. 7B). These results further support the concept that the cCHP-PspA vaccine formulation is an attractive inhalant delivery vehicle that effectively delivers and sustains antigen at the nasal epithelium for continuous antigen uptake by DCs without antigen deposition in the CNS.

DISCUSSION

We showed that cCHP-PspA-vaccinated mice survived a lethal challenge with *S. pneumoniae* (Fig. 1; see Fig. S4 in the supplemental material), whereas mice vaccinated with cCHP complexed with an irrelevant antigen (BoHc/A) did not (see Fig. S3 and S4). Importantly, compared with those of mice inoculated with control constructs, the respiratory tracts of mice immunized with intranasal cCHP-PspA had less colonization and invasion by pneumococcal organisms (Fig. 2 and 3). Intranasal administration of cCHP-PspA resulted in enhanced PspA-specific Th17 responses (Fig. 4A) and mucosal IgA and systemic IgG antibody responses (Fig. 5 and 6), all of which are involved in establishing protective immunity against pneumococci (10, 28–30). To our knowledge, the current study is the first to show the efficacy of a nasal vaccine not only for inducing protective immune responses but also for preventing nasal colonization by use of a single protein antigen (PspA) without adding any biologically active adjuvant.

The precise mechanisms underlying the efficacy of cCHP-PspA as a nasal vaccine against *S. pneumoniae* lung infection remain to be elucidated. However, we speculate that serum and BALF IgGs, the main isotype of antibody induced by the cCHP-PspA nasal vaccine in the lower respiratory compartment (Fig. 5A and 6D), play key roles in survival against lethal challenge with *S. pneumoniae*, given that antibody titers of PspA-specific IgA in the BALF were low (Fig. 6B) and therefore might contribute only minimally to protection against invasive diseases. This hypothesis is supported by the results of a previous study (28) in which $IgA^{-/-}$ mice immunized with intranasal PspA-adjuvant (i.e., a plasmid expressing Flt3 ligand cDNA) mounted a protective immune response against lethal challenge with *S. pneumoniae*. Our current study shows that the cCHP-PspA nasal vaccine effectively induced antigen-specific sIgA antibodies in the upper airways (Fig. 6A). Immunization of $IgA^{-/-}$ mice with intranasal PspA-adjuvant did not prevent pneumococcal colonization of the nasal cavity (28). In light of the findings of the previous study (28) and our current one, serum antigen-specific IgG antibodies are crucial to preventing invasive disease associated with clinical signs, whereas antigen-specific sIgA antibodies are essential for preventing colonization of the upper respiratory tract by *S. pneumoniae*.

In addition to the essential role of sIgA in protection from nasopharyngeal colonization by pneumococci, IL-17A-producing $CD4^+$ T cells play an important role in preventing pneumococcal nasal colonization in mice immunized with intranasal pneumococcal whole-cell antigen (29, 30). Recent studies have found that IL-17 promotes multiple aspects of humoral immunity by enhancing B cell proliferation and isotype switching (51), B cell recruitment to the respiratory mucosa, and expression of the polymeric immunoglobulin receptor on the airway epithelium (52). In the current study, we found that intranasal immunization with cCHP-PspA generated Th17 cells in the nasal passages, draining lymph nodes, and systemic compartment (Fig. 4A). Therefore, our findings suggest that intranasal immunization with cCHP-PspA induces both humoral and cellular immune responses, which are required for protective immunity against pneumococcal colonization and invasive disease. In addition to their essential role in antipneumococcal immunity (29, 30), Th17 responses are a hallmark of autoimmunity (53). Therefore, future studies should carefully examine whether the Th17 responses induced by intranasal immunization with cCHP-PspA are associated with any adverse effects.

As one might expect, the protective immunity induced by nasal cCHP-PspA was not observed when an irrelevant antigen, BoHc/A, was incorporated into cCHP (cCHP-BoHc/A) (35) and used as a nasal vaccine (see Fig. S3 and S4 in the supplemental material). Moreover, mice immunized intranasally with cCHP-PspA (PspA of clades 1 and 2) were protected against challenge with pneumococcal strain 3JYP3670, which expresses PspA of clade 4 (10), whereas mice immunized with cCHP-BoHc/A, PspA

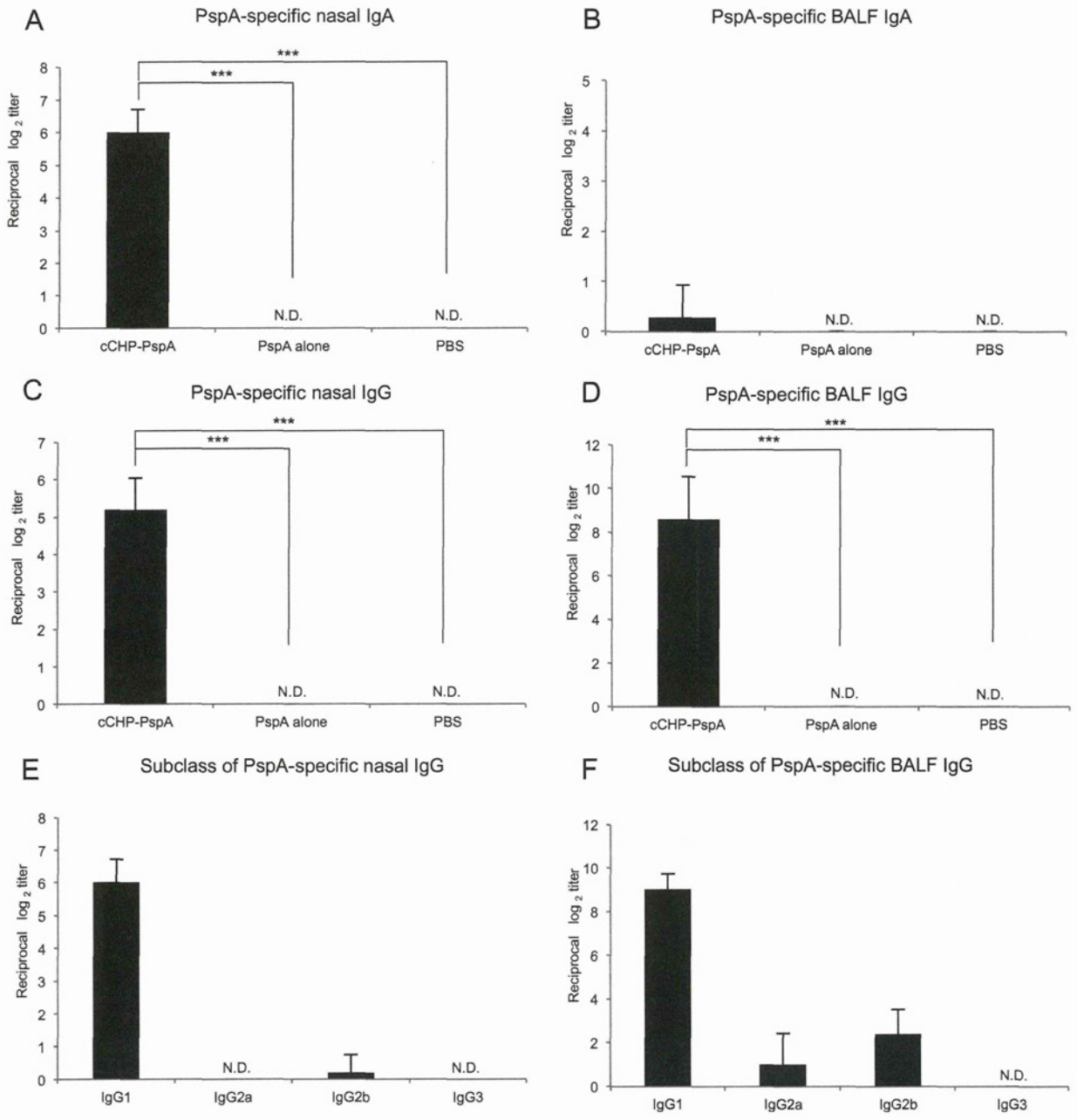

FIG 6 Intranasal vaccination with cCHP-PspA induced strong PspA-specific secretory IgA and IgG responses. Titers of nasal (A and C) and bronchial (B and D) IgA and IgG induced by intranasal immunization with PspA alone or PspA mixed with cCHP are shown. Titers of PspA-specific IgA and IgG in nasal washes and BALFs were measured on day 7 after final immunization. Intranasal cCHP-PspA vaccination induced high levels of IgG1 and IgG2b in mucosal secretions of the upper (E) and lower (F) airways. Data are representative of five independent experiments, and each group consisted of 5 mice. N.D., not detected in undiluted samples. ***, $P < 0.001$. Abbreviations: BALF, bronchoalveolar lavage fluid; cCHP, cationic cholesteryl-group-bearing pullulan; Ig, immunoglobulin; PspA, pneumococcal surface protein A.

alone, or PBS were not (see Fig. S4). These findings highlight the potential advantage of nasal vaccination of cCHP-PspA in inducing antigen-specific protective immunity with subtype cross-reactivity.

Note that cCHP lacks any biologically active adjuvant effect because it cannot activate immune cells by itself (35). The nanogel formulation had no effect on the expression of costimulatory molecules on nasal DCs (see Fig. S5 in the supplemental material), which are supposed to already express high steady-state levels of costimulatory molecules in the mucosal environment in response to numerous inhaled antigens. Our current and previous studies have shown that antigens are released from the nanogel and are taken up efficiently by DCs in the nasal mucosa (Fig. 7B) (35). These studies suggest that cCHP nanogel is an effective carrier that has strong chaperone-like activity, enabling the delivery of PspA across the nasal mucosal epithelial cell layer for subsequent uptake by DCs and initiation of antigen-specific immune responses.

In summary, this study introduced a promising nanometer-

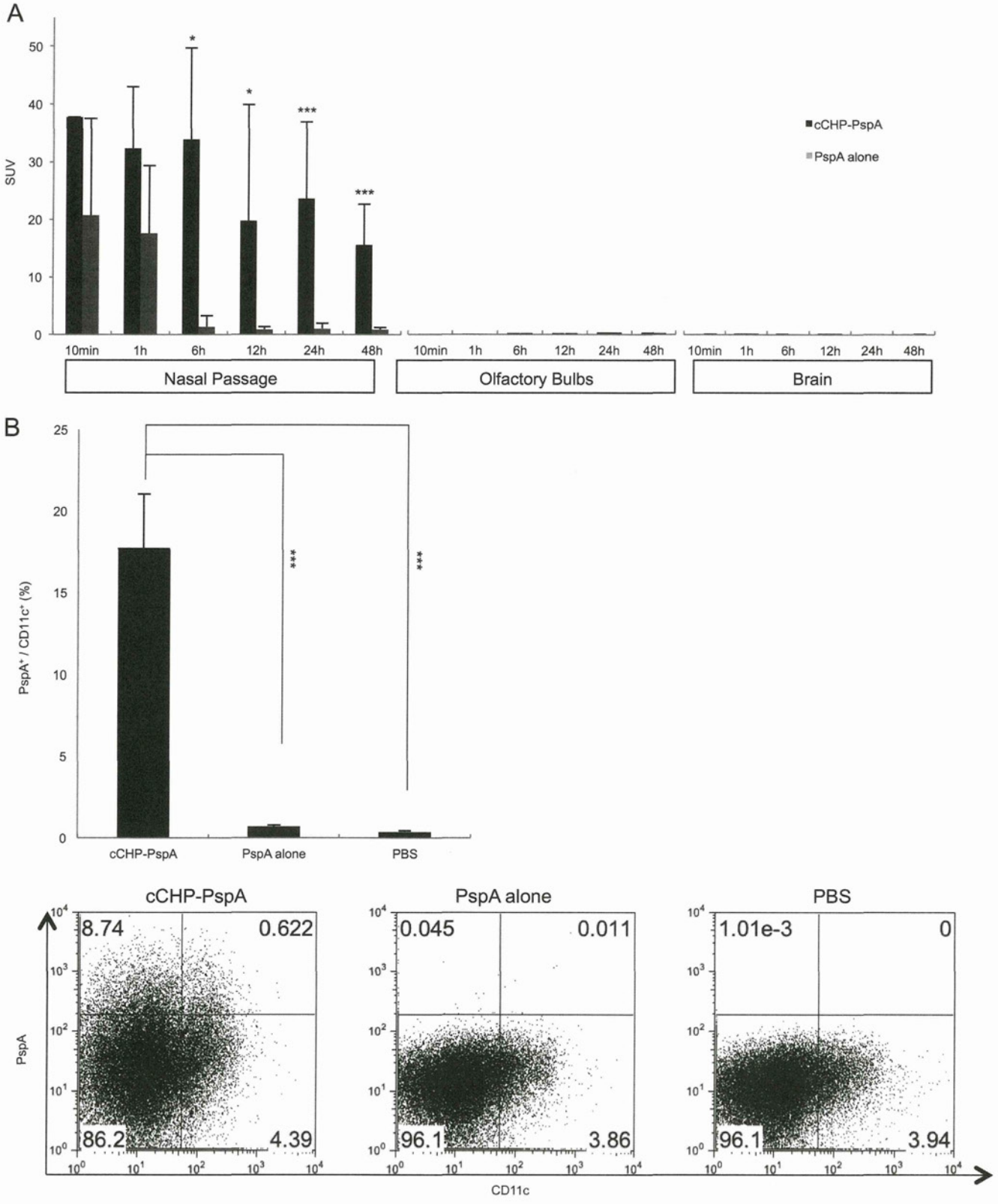

FIG 7 Intranasal vaccination with cCHP-PspA induced no accumulation of PspA in the central nervous system (A) but enhanced the efficiency of uptake of PspA by dendritic cells in the nasal passages (B). (A) ^{111}In-labeled PspA was administered intranasally with or without cCHP nanogel, and the radioisotope counts (SUVs) in the nasal passages, olfactory bulbs, and brain were estimated 10 min and 1, 6, 12, 24, and 48 h after instillation. (B) Dendritic cells in the nasal passages of mice immunized intranasally with cCHP-PspA, PspA alone, or PBS were analyzed by flow cytometry 6 h after immunization. Data are representative of three independent experiments, and each group consisted of 5 mice. *, $P < 0.05$; ***, $P < 0.001$. Abbreviations: cCHP, cationic cholesteryl group-bearing pullulan; PspA, pneumococcal surface protein A.

sized carrier-based pneumococcal nasal vaccine that incorporates cCHP nanogel and the pneumococcal serotype-independent protein antigen PspA. The antigen-specific immune responses induced by this vaccine effectively protected mice against the respiratory pathogen *S. pneumoniae*. Our results confirmed that cCHP nanogel is a promising candidate carrier of a protein antigen for a mucosal vaccine that induces humoral and cellular immune responses against PspA to combat colonization and invasion of the airways by respiratory pathogens.

ACKNOWLEDGMENTS

This study was supported by a grant-in-aid from the Research Fellowship of the Japan Society for the Promotion of Science (JSPS) (I.G.K., A.S., and T.N.); by programs of special coordination funds for promoting science and technology, a grant-in-aid for scientific research on priority areas, and a grant-in-aid for scientific research from the Ministry of Education, Culture, Sports, Science, and Technology of Japan (J.K. and H.K.); by the Ministry of Health, Labor, and Welfare of Japan (J.K., Y.Y., and H.K.); by the New Energy and Industrial Technology Development Organization (NEDO) (Y.Y. and H.K.); by the Young Researcher Overseas Visits Program for Vitalizing Brain Circulation of the Japan Society for the Promotion of Science (J.K., H.K., and Y.Y.); by the Program for Promotion of Basic and Applied Researches for Innovations in Bio-Oriented Industry (BRAIN) (T.N., S. Sato, and J.K.); by the Yakult Bio-Science Foundation (J.K.); and by the Global Center of Excellence Program "Center of Education and Research for Advanced Genome-Based Medicine—For Personalized Medicine and the Control of Worldwide Infectious Diseases" (H.K.).

We declare that we have no conflicts of interest.

REFERENCES

1. **Dinleyici EC, Yargic ZA.** 2008. Pneumococcal conjugated vaccines: impact of PCV-7 and new achievements in the postvaccine era. Expert Rev. Vaccines **7**:1367–1394.
2. **Rose M, Zielen S.** 2009. Impact of infant immunization programs with pneumococcal conjugate vaccine in Europe. Expert Rev. Vaccines **8**:1351–1364.
3. **Principi N, Esposito S.** 2012. Use of the 13-valent pneumococcal conjugate vaccine in infants and young children. Expert Opin. Biol. Ther. **12**: 641–648.
4. **Huang SS, Johnson KM, Ray GT, Wroe P, Lieu TA, Moore MR, Zell ER, Linder JA, Grijalva CG, Metlay JP, Finkelstein JA.** 2011. Healthcare utilization and cost of pneumococcal disease in the United States. Vaccine **29**:3398–3412.
5. **Thigpen MC, Whitney CG, Messonnier NE, Zell ER, Lynfield R, Hadler JL, Harrison LH, Farley MM, Reingold A, Bennett NM, Craig AS, Schaffner W, Thomas A, Lewis MM, Scallan E, Schuchat A.** 2011. Bacterial meningitis in the United States, 1998–2007. N. Engl. J. Med. **364**:2016–2025.
6. **Weinberger DM, Malley R, Lipsitch M.** 2011. Serotype replacement in disease after pneumococcal vaccination. Lancet **378**:1962–1973.
7. **Hsu HE, Shutt KA, Moore MR, Beall BW, Bennett NM, Craig AS, Farley MM, Jorgensen JH, Lexau CA, Petit S, Reingold A, Schaffner W, Thomas A, Whitney CG, Harrison LH.** 2009. Effect of pneumococcal conjugate vaccine on pneumococcal meningitis. N. Engl. J. Med. **360**: 244–256.
8. **Singleton RJ, Hennessy TW, Bulkow LR, Hammitt LL, Zulz T, Hurlburt DA, Butler JC, Rudolph K, Parkinson A.** 2007. Invasive pneumococcal disease caused by nonvaccine serotypes among Alaska native children with high levels of 7-valent pneumococcal conjugate vaccine coverage. JAMA **297**:1784–1792.
9. **Briles DE, Hollingshead SK, Nabors GS, Paton JC, Brooks-Walter A.** 2000. The potential for using protein vaccines to protect against otitis media caused by *Streptococcus pneumoniae*. Vaccine **19**(Suppl 1):S87–S95.
10. **Briles DE, Hollingshead SK, King J, Swift A, Braun PA, Park MK, Ferguson LM, Nahm MH, Nabors GS.** 2000. Immunization of humans with recombinant pneumococcal surface protein A (rPspA) elicits antibodies that passively protect mice from fatal infection with *Streptococcus pneumoniae* bearing heterologous PspA. J. Infect. Dis. **182**:1694–1701.
11. **Briles DE, Hollingshead SK, Paton JC, Ades EW, Novak L, van Ginkel FW, Benjamin Jr, WH.** 2003. Immunizations with pneumococcal surface protein A and pneumolysin are protective against pneumonia in a murine model of pulmonary infection with *Streptococcus pneumoniae*. J. Infect. Dis. **188**:339–348.
12. **Briles DE, Tart RC, Swiatlo E, Dillard JP, Smith P, Benton KA, Ralph BA, Brooks-Walter A, Crain MJ, Hollingshead SK, McDaniel LS.** 1998. Pneumococcal diversity: considerations for new vaccine strategies with emphasis on pneumococcal surface protein A (PspA). Clin. Microbiol. Rev. **11**:645–657.
13. **Olafsdottir TA, Lingnau K, Nagy E, Jonsdottir I.** 2012. Novel protein-based pneumococcal vaccines administered with the Th1-promoting adjuvant IC31 induce protective immunity against pneumococcal disease in neonatal mice. Infect. Immun. **80**:461–468.
14. **Hollingshead SK, Becker R, Briles DE.** 2000. Diversity of PspA: mosaic genes and evidence for past recombination in *Streptococcus pneumoniae*. Infect. Immun. **68**:5889–5900.
15. **Crain MJ, Waltman WD, 2nd, Turner JS, Yother J, Talkington DF, McDaniel LS, Gray BM, Briles DE.** 1990. Pneumococcal surface protein A (PspA) is serologically highly variable and is expressed by all clinically important capsular serotypes of *Streptococcus pneumoniae*. Infect. Immun. **58**:3293–3299.
16. **McDaniel LS, Sheffield JS, Delucchi P, Briles DE.** 1991. PspA, a surface protein of *Streptococcus pneumoniae*, is capable of eliciting protection against pneumococci of more than one capsular type. Infect. Immun. **59**:222–228.
17. **Tart RC, McDaniel LS, Ralph BA, Briles DE.** 1996. Truncated *Streptococcus pneumoniae* PspA molecules elicit cross-protective immunity against pneumococcal challenge in mice. J. Infect. Dis. **173**:380–386.
18. **Xin W, Li Y, Mo H, Roland KL, Curtiss R.** 2009. PspA family fusion proteins delivered by attenuated *Salmonella enterica* serovar Typhimurium extend and enhance protection against *Streptococcus pneumoniae*. Infect. Immun. **77**:4518–4528.
19. **Nabors GS, Braun PA, Herrmann DJ, Heise ML, Pyle DJ, Gravenstein S, Schilling M, Ferguson LM, Hollingshead SK, Briles DE, Becker RS.** 2000. Immunization of healthy adults with a single recombinant pneumococcal surface protein A (PspA) variant stimulates broadly cross-reactive antibodies to heterologous PspA molecules. Vaccine **18**:1743–1754.
20. **Gray BM, Converse GM, 3rd, Dillon HC, Jr.** 1980. Epidemiologic studies of *Streptococcus pneumoniae* in infants: acquisition, carriage, and infection during the first 24 months of life. J. Infect. Dis. **142**:923–933.
21. **Faden H, Duffy L, Wasielewski R, Wolf J, Krystofik D, Tung Y.** 1997. Relationship between nasopharyngeal colonization and the development of otitis media in children. J. Infect. Dis. **175**:1440–1445.
22. **Leiberman A, Dagan R, Leibovitz E, Yagupsky P, Fliss DM.** 1999. The bacteriology of the nasopharynx in childhood. Int. J. Pediatr. Otorhinolaryngol. **49**(Suppl 1):S151–S153.
23. **Hoge CW, Reichler MR, Dominguez EA, Bremer JC, Mastro TD, Hendricks KA, Musher DM, Elliott JA, Facklam RR, Breiman RF.** 1994. An epidemic of pneumococcal disease in an overcrowded, inadequately ventilated jail. N. Engl. J. Med. **331**:643–648.
24. **Wu HY, Nahm MH, Guo Y, Russell MW, Briles DE.** 1997. Intranasal immunization of mice with PspA (pneumococcal surface protein A) can prevent intranasal carriage, pulmonary infection, and sepsis with *Streptococcus pneumoniae*. J. Infect. Dis. **175**:839–846.
25. **Yamamoto M, Briles DE, Yamamoto S, Ohmura M, Kiyono H, McGhee JR.** 1998. A nontoxic adjuvant for mucosal immunity to pneumococcal surface protein A. J. Immunol. **161**:4115–4121.
26. **Briles DE, Ades E, Paton JC, Sampson JS, Carlone GM, Huebner RC, Virolainen A, Swiatlo E, Hollingshead SK.** 2000. Intranasal immunization of mice with a mixture of the pneumococcal proteins PsaA and PspA is highly protective against nasopharyngeal carriage of *Streptococcus pneumoniae*. Infect. Immun. **68**:796–800.
27. **Oma K, Zhao J, Ezoe H, Akeda Y, Koyama S, Ishii KJ, Kataoka K, Oishi K.** 2009. Intranasal immunization with a mixture of PspA and a Toll-like receptor agonist induces specific antibodies and enhances bacterial clearance in the airways of mice. Vaccine **27**:3181–3188.
28. **Fukuyama Y, King JD, Kataoka K, Kobayashi R, Gilbert RS, Oishi K, Hollingshead SK, Briles DE, Fujihashi K.** 2010. Secretory-IgA antibodies play an important role in the immunity to *Streptococcus pneumoniae*. J. Immunol. **185**:1755–1762.
29. **Lu YJ, Gross J, Bogaert D, Finn A, Bagrade L, Zhang Q, Kolls JK, Srivastava A, Lundgren A, Forte S, Thompson CM, Harney KF, An-**

derson PW, Lipsitch M, Malley R. 2008. Interleukin-17A mediates acquired immunity to pneumococcal colonization. PLoS Pathog. 4:e1000159. doi:10.1371/journal.ppat.1000159.
30. Malley R. 2005. $CD4^+$ T cells mediate antibody-independent acquired immunity to pneumococcal colonization. Proc. Natl. Acad. Sci. U. S. A. 102:4848–4853.
31. Xu-Amano J, Kiyono H, Jackson RJ, Staats HF, Fujihashi K, Burrows PD, Elson CO, Pillai S, McGhee JR. 1993. Helper T cell subsets for immunoglobulin A responses: oral immunization with tetanus toxoid and cholera toxin as adjuvant selectively induces Th2 cells in mucosa associated tissues. J. Exp. Med. 178:1309–1320.
32. Freytag LC, Clements JD. 2005. Mucosal adjuvants. Vaccine 23:1804–1813.
33. Mutsch M, Zhou W, Rhodes P, Bopp M, Chen RT, Linder T, Spyr C, Steffen R. 2004. Use of the inactivated intranasal influenza vaccine and the risk of Bell's palsy in Switzerland. N. Engl. J. Med. 350:896–903.
34. van Ginkel FW, Jackson RJ, Yuki Y, McGhee JR. 2000. Cutting edge: the mucosal adjuvant cholera toxin redirects vaccine proteins into olfactory tissues. J. Immunol. 165:4778–4782.
35. Nochi T, Yuki Y, Takahashi H, Sawada S, Mejima M, Kohda T, Harada N, Kong IG, Sato A, Kataoka N, Tokuhara D, Kurokawa S, Takahashi Y, Tsukada H, Kozaki S, Akiyoshi K, Kiyono H. 2010. Nanogel antigenic protein-delivery system for adjuvant-free intranasal vaccines. Nat. Mater. 9:572–578.
36. Reference deleted.
37. Ayame H, Morimoto N, Akiyoshi K. 2008. Self-assembled cationic nanogels for intracellular protein delivery. Bioconjug. Chem. 19:882–890.
38. Kurono Y, Yamamoto M, Fujihashi K, Kodama S, Suzuki M, Mogi G, McGhee JR, Kiyono H. 1999. Nasal immunization induces *Haemophilus influenzae*-specific Th1 and Th2 responses with mucosal IgA and systemic IgG antibodies for protective immunity. J. Infect. Dis. 180:122–132.
39. Darrieux M, Miyaji EN, Ferreira DM, Lopes LM, Lopes AP, Ren B, Briles DE, Hollingshead SK, Leite LC. 2007. Fusion proteins containing family 1 and family 2 PspA fragments elicit protection against *Streptococcus pneumoniae* that correlates with antibody-mediated enhancement of complement deposition. Infect. Immun. 75:5930–5938.
40. Francis KP, Yu J, Bellinger-Kawahara C, Joh D, Hawkinson MJ, Xiao G, Purchio TF, M. Caparon G, Lipsitch M, Contag PR. 2001. Visualizing pneumococcal infections in the lungs of live mice using bioluminescent *Streptococcus pneumoniae* transformed with a novel gram-positive *lux* transposon. Infect. Immun. 69:3350–3358.
41. Kadurugamuwa JL, Modi K, Coquoz O, Rice B, Smith S, Contag PR, Purchio T. 2005. Reduction of astrogliosis by early treatment of pneumococcal meningitis measured by simultaneous imaging, in vivo, of the pathogen and host response. Infect. Immun. 73:7836–7843.
42. Michel RB, Andrews PM, Castillo ME, Mattes MJ. 2005. *In vitro* cytotoxicity of carcinoma cells with ^{111}In-labeled antibodies to HER-2. Mol. Cancer Ther. 4:927–937.
43. Fukuyama S, Hiroi T, Yokota Y, Rennert PD, Yanagita M, Kinoshita N, Terawaki S, Shikina T, Yamamoto M, Kurono Y, Kiyono H. 2002. Initiation of NALT organogenesis is independent of the IL-7R, LTβR, and NIK signaling pathways but requires the Id2 gene and $CD3^-CD4^+CD45^+$ cells. Immunity 17:31–40.
44. Hollingshead SK. 2006. Pneumococcal surface protein A (PspA) family distribution among clinical isolates from adults over 50 years of age collected in seven countries. J. Med. Microbiol. 55:215–221.
45. Ren B, Szalai AJ, Hollingshead SK, Briles DE. 2004. Effects of PspA and antibodies to PspA on activation and deposition of complement on the pneumococcal surface. Infect. Immun. 72:114–122.
46. Beall B, Gherardi G, Facklam RR, Hollingshead SK. 2000. Pneumococcal PspA sequence types of prevalent multiresistant pneumococcal strains in the United States and of internationally disseminated clones. J. Clin. Microbiol. 38:3663–3669.
47. Brandileone M. 2004. Typing of pneumococcal surface protein A (PspA) in *Streptococcus pneumoniae* isolated during epidemiological surveillance in Brazil: towards novel pneumococcal protein vaccines. Vaccine 22:3890–3896.
48. Mollerach M, Regueira M, Bonofiglio L, Callejo R, Pace J, Di Fabio JL, Hollingshead SK, Briles DE. 2004. Invasive *Streptococcus pneumoniae* isolates from Argentinian children: serotypes, families of pneumococcal surface protein A (PspA) and genetic diversity. Epidemiol. Infect. 132:177–184.
49. Vela Coral MC, Fonseca N, Castaneda E, Di Fabio JL, Hollingshead SK, Briles DE. 2001. Pneumococcal surface protein A of invasive *Streptococcus pneumoniae* isolates from Colombian children. Emerg. Infect. Dis. 7:832–836.
50. Dubin PJ, Kolls JK. 2009. Interleukin-17A and interleukin-17F: a tale of two cytokines. Immunity 30:9–11.
51. Doreau A, Belot A, Bastid J, Riche B, Trescol-Biemont MC, Ranchin B, Fabien N, Cochat P, Pouteil-Noble C, Trolliet P, Durieu I, Tebib J, Kassai B, Ansieau S, Puisieux A, Eliaou JF, Bonnefoy-Berard N. 2009. Interleukin 17 acts in synergy with B cell-activating factor to influence B cell biology and the pathophysiology of systemic lupus erythematosus. Nat. Immunol. 10:778–785.
52. Jaffar Z, Ferrini ME, Herritt LA, Roberts K. 2009. Cutting edge: lung mucosal Th17-mediated responses induce polymeric Ig receptor expression by the airway epithelium and elevate secretory IgA levels. J. Immunol. 182:4507–4511.
53. Bettelli E, Oukka M, Kuchroo VK. 2007. Th17 cells in the circle of immunity and autoimmunity. Nat. Immunol. 8:345–350.

Transcription factor Spi-B–dependent and –independent pathways for the development of Peyer's patch M cells

S Sato[1,2], S Kaneto[1,3], N Shibata[1,4], Y Takahashi[1], H Okura[1,4], Y Yuki[1], J Kunisawa[1,4,5] and H Kiyono[1,2,3,4,6]

Although many of the biological features of microfold cells (M cells) have been known for many years, the molecular mechanisms of M-cell development and antigen recognition have remained unclear. Here, we report that *Umod* is a novel M-cell–specific gene, the translation products of which might contribute to the uptake function of M cells. Transcription factor Spi-B was also specifically expressed in M cells among non-hematopoietic lineages. Spi-B–deficient mice showed reduced expression of most, but not all, other M-cell–specific genes and M-cell surface markers. Whereas uptake of *Salmonella* Typhimurium via M cells was obviously reduced in Spi-B–deficient mice, the abundance of intratissue cohabiting bacteria was comparable between wild-type and Spi-B–deficient mice. These data indicate that there is a small M-cell population with developmental regulation that is Spi-B independent; however, Spi-B is probably a candidate master regulator of M-cell functional maturation and development by another pathway.

INTRODUCTION

Mucosa-associated lymphoid tissues, represented in the small intestine by Peyer's patches (PPs), are the inductive sites of the mucosal immune system.[1] Unlike other peripheral lymphoid tissues, mucosa-associated lymphoid tissues do not have afferent vessels; instead, they have a direct antigen-sampling system that takes antigens into the tissue from the mucosal surface. This antigen uptake is managed mainly by microfold cells (M cells), which are located within the follicle-associated epithelium (FAE) of mucosa-associated lymphoid tissues and are regarded as professional antigen-sampling cells.[1] M cells have unique morphological features, such as relatively short, irregular microvilli on their apical surfaces and a pocket structure on their basolateral side that enfolds lymphocytes and antigen-presenting cells. These distinctive features are considered to contribute to M-cell functions: the short microvilli enable easy contact with luminal antigens, and the ability to hold antigen-presenting cells, such as dendritic cells, in their pockets is valuable for the prompt transfer of antigens to dendritic cells for speedy initiation of antigen-specific mucosal immunity. Because M cells are principal targets for effective peroral vaccination, elucidation of the molecular mechanisms behind their antigen-uptake functions and differentiation is important for the development of new-era oral vaccines.

We have reported that glycoprotein 2 (GP2) is specifically expressed on M cells,[2] and a progressive study has demonstrated that GP2 acts as a binding receptor for FimH-expressing bacteria, inducing effective uptake of, and specific immune responses to, such bacteria.[3] Although several other M-cell–specific molecules, such as MARCKS-like protein,[2] peptidoglycan recognition protein S,[4] and fucosyltransferase 1 (FUT1),[5] have been reported, the functions of these molecules in contributing to antigen uptake have not yet been revealed. In addition, the mechanisms of M-cell differentiation are poorly understood.

Recently, it has been reported that the intestinal epithelial crypt–villus structure can be assembled from a single Lgr5-positive stem cell in the absence of a non-epithelial-cell niche.[6] It has also been reported that almost all small intestinal epithelial cell (EC) lineages develop from intestinal epithelial

[1]Division of Mucosal Immunology, Department of Microbiology and Immunology, The Institute of Medical Science, The University of Tokyo, Tokyo, Japan. [2]Core Research for Evolutional Science and Technology (CREST), Japan Science and Technology Agency, Tokyo, Japan. [3]Graduate School of Medicine, The University of Tokyo, Tokyo, Japan. [4]Department of Medical Genome Science, Graduate School of Frontier Science, The University of Tokyo, Chiba, Japan. [5]Laboratory of Vaccine Materials, National Institute of Biomedical Innovation, Osaka, Japan and [6]International Research and Development Center for Mucosal Vaccines, The Institute of Medical Science, The University of Tokyo, Tokyo, Japan. Correspondence: H Kiyono (kiyono@ims.u-tokyo.ac.jp)

Received 16 July 2012; accepted 1 November 2012; advance online publication 5 December 2012. doi:10.1038/mi.2012.122

stem cells. First, the expression of Math1 transcription factor determines the destiny of stem cells for the secretory lineage.[7] Further differentiation of secretory lineage cells, such as goblet cells, Paneth cells, and endocrine cells, requires other factors such as Klf4, Sox9, and Ngn3, respectively.[8–11] On the other hand, if the stem cells express Hes1, which inhibits Math1 expression, these cells adopt a non-secretory lineage and become, for example, enterocytes.[12] Because M cells belong to a non-secretory lineage, at least one unknown factor might be expressed and activated downstream of Hes1 in precursor cells for differentiation into M cells.

Here, we report the existence of two additional M-cell–specific genes among mouse intestinal ECs, as determined from the data obtained in our previously reported DNA gene chip analysis.[2] One is *Umod*, which encodes the cell-surface expression molecule Tamm–Horsfall protein (THP). The other one, *Spib*, encodes Spi-B, which is a transcription factor belonging to the Ets family. In focusing on the function of Spi-B, our investigations revealed that M-cell–intrinsic Spi-B controls the expression of other, but not all, M-cell–specific genes. In addition, Spi-B regulates the ultrastructural development and GP2-mediated antigen-uptake functions of most PP M cells, whereas a translocation of the majority of *Alcaligenes* spp., which are commensal bacteria resident in PPs and isolated lymphoid follicles preferentially through M cells, was observed independently of Spi-B. We propose that M-cell–intrinsic Spi-B is an essential transcription factor for the functional and structural differentiation of M cells, although a small population of M cells may mature independently of Spi-B. These M cells, which were found within the FAE of Spi-B–deficient mice, might still be present in sufficient numbers to contribute to the migration of mucosa-associated lymphoid tissue-resident bacteria.

RESULTS

Spib and *Umod* are expressed in M cells but not other intestinal ECs

We previously reported the discovery of a series of PP M-cell–specific genes by DNA gene chip analysis.[2] To search for other M-cell–specific molecules—especially a key transcription factor for M-cell development or function—we used real-time polymerase chain reaction (PCR) to screen candidate genes from gene chip analysis data. Whole ECs and lymphocytes were prepared from well-trimmed duodenal PPs as "PP ECs" and "PP lymphocytes," respectively. PP M cells and non-M cells were then purified from PP ECs as NKM 16-2-4 antibody (NKM)/*Ulex europaeus* agglutinin 1 (UEA-1) double-positive and double-negative cells, respectively.[13] Among several candidates, we confirmed that *Spib* and *Umod* were preferentially expressed in PP M cells (**Figure 1a**). We next performed an *in situ* hybridization analysis of *Spib* and *Umod* expressions in PPs to confirm the real-time PCR data. An antisense cRNA probe for *Spib* specifically stained part of the FAE region of the PP among the intestinal ECs (**Figure 1b**) and (as was expect from the previous studies[14,15]) in the lymphocyte region of the PPs, especially in the germinal centers (**Figure 1b,c**, dotted circles). Similarly, *Umod* expression was observed within the FAE region. A negative control experiment using each sense probe gave no signals for either *Spib* or *Umod*. In addition, expression of both *Spib* and *Umod* was well colocalized with UEA-1–positive cells (**Figure 1c**). These findings demonstrated that *Spib* and *Umod* were expressed in PP M cells but not in other intestinal ECs.

Expression of M-cell–specific surface markers is severely diminished in Spi-B–deficient mice

Expression of *Spib* in PP M cells was high—at levels comparable to that of *Gp2* and *Marcksl1*, which were previously reported to be M-cell–specific genes.[2] In addition, because Spi-B is a transcription factor belonging to the Ets family, it is probable that it controls the expression of genes encoding molecules that contribute to M-cell function or development, or both. Therefore, we decided to focus our efforts on investigating an *in vivo* role of Spi-B in M cells. Spi-B–deficient ($Spib^{-/-}$) mice[15] were thus employed and the characteristics of their PP M cells were compared with those of wild-type ($Spib^{+/+}$) mice.

GP2 is expressed on M cells and not on other intestinal ECs;[2,3] therefore, we first examined GP2 expression by using whole-mount staining. In wild-type mice, GP2 expression was clearly and specifically detected in the FAE region (**Figure 2a**), as demonstrated previously.[2,3] In contrast, $Spib^{-/-}$-derived PPs completely lost their GP2 expression, as found in $Gp2^{-/-}$-derived PPs[3] (**Figure 2b**). More classically, mouse PP M cells were defined as NKM antibody (and/or UEA-1)–positive and wheat germ agglutinin–negative (NKM^+WGA^-) FAE cells,[13] as seen in the PPs from $Spib^{+/+}$ mice (**Figure 2c**). $Spib^{-/-}$-derived PPs showed reduced numbers of NKM^+WGA^- cells (**Figure 2d–f**); these cells are considered to have the hallmarks of M cells. Notably, although GP2-positive FAE cells were completely abolished in $Spib^{-/-}$ mice (**Figure 2b**), a few NKM^+WGA^- cells were found in $Spib^{-/-}$-derived PPs (**Figure 2e,f**; about 10 per FAE region vs. about 350 per FAE region in the case of $Spib^{+/+}$ cells).

Gp2 is a target gene of Spi-B

Because GP2 is a highly glycosylated protein and the anti-mouse GP2 antibody used in this research (clone 2F11-C3) was raised against recombinant mouse GP2-Fc fusion protein produced by mammalian cells,[3] it was possible that recognition of GP2 by 2F11-C3 antibody depended on glycosylation. Hence, we next checked the expression level of *Gp2* transcript in the FAE region by using quantitative real-time PCR. Consistent with the whole-mount staining data, *Gp2* expression was dramatically suppressed in $Spib^{-/-}$ mice-derived FAE (**Figure 3a**), indicating that *Gp2* expression is exclusively regulated by Spi-B.

UEA-1 and NKM antibody recognize α (1,2)-fucose, which specifically binds the terminal galactose residues of some surface membrane proteins.[13] Given that terminal fucosylation on PP M cells is catalyzed by FUT1, which is coded by the M-cell–specific gene *Fut1* (Terahara *et al.*[5] and **Supplementary Figure S1** online), the cause of the decrease in numbers of NKM^+WGA^- cells in the FAE of $Spib^{-/-}$ mice might have

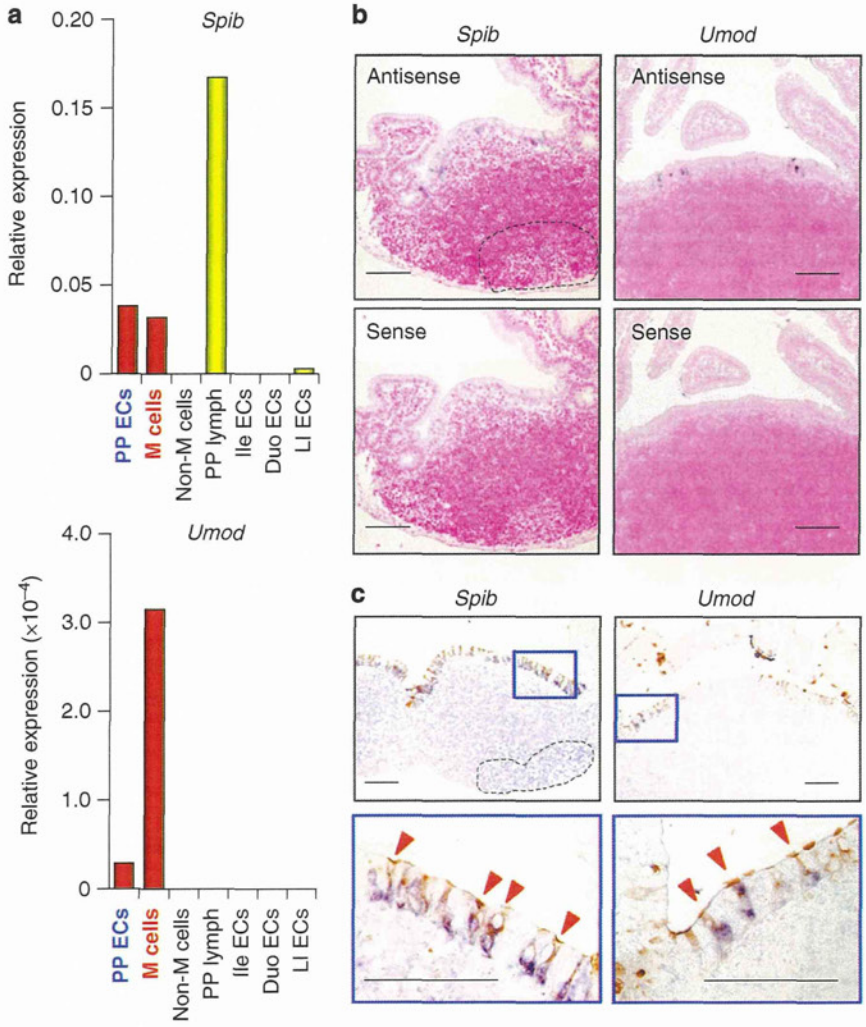

Figure 1 M cells are unique among intestinal epithelial cells in showing expression of *Spib* and *Umod*. (**a**) Real-time PCR analysis of the expression of newly identified M-cell–specific genes in the cell fractions indicated. Each result was normalized against the expression of glyceraldehyde 3-phosphate dehydrogenase (*Gapdh*) and is representative of three independent experiments. Lymph, lymphocytes; Ile, ileal; Duo, duodenal; LI, large intestinal. (**b**) *In situ* hybridization assay to detect *Spib* and *Umod* mRNA in a duodenal PP. Each antisense, but not sense, cRNA probes reacted with FAE regions to give a blue stain. Bar = 100 μm. (**c**) *Spib* and *Umod* signals were merged with brown UEA-1 staining in the FAE region. Each bottom panel is a higher magnification of the blue square in each top panel. Dotted circles found in **b** and **c** indicated germinal center region of PPs. Data are representative of two independent experiments. Bar = 100 μm.

simply been impairment of fucosylation on some M-cell–specific surface molecules. To test this possibility, we assessed the expression of *Fut1* mRNA in the FAE region. Unexpectedly, the levels of *Fut1* expression were comparable in $Spib^{+/+}$ and $Spib^{-/-}$ mice (**Figure 3b**). We further examined the expression of other M-cell–specific genes, including *Umod*, in $Spib^{+/+}$ and $Spib^{-/-}$ mice. Although *Umod*, like *Gp2*, was poorly expressed in $Spib^{-/-}$ FAE, the expression levels of *Marcksl1* (which encodes MARCKS-like protein) and *Pglyrp1* (which encodes peptidoglycan recognition protein S) in the FAE region of $Spib^{-/-}$ mice were similar to those in wild-type mice (**Figure 3c**). These results indicated that M-cell–specific expression molecules could be divided into two groups according to their dependence on Spi-B for gene regulation.

Abundance of cells with irregular and short microvilli is diminished in $Spib^{-/-}$ PPs

M cells are easily distinguished from the neighboring columnar ECs by their morphologically unique surface microvilli, which are sparser and shorter. It is likely that these irregular microvilli are convenient for the effective uptake of ingested antigens from luminal sites in the digestive tract. Therefore, this feature is another hallmark of M cells. We prepared PPs from $Spib^{+/+}$ and $Spib^{-/-}$ mice and then observed and counted hollow cells by scanning electron microscopy. M cells were preferentially found at the edge of the FAE region in wild-type mice as "sunken" cells (**Figure 4a,b**; about 35 sunken cells per 0.01-mm^2 field). In contrast, these sunken cells were rarely detected (about 3 sunken cells per 0.01-mm^2 field) in the corresponding region of $Spib^{-/-}$ mice. Notably, however, a pocket structure

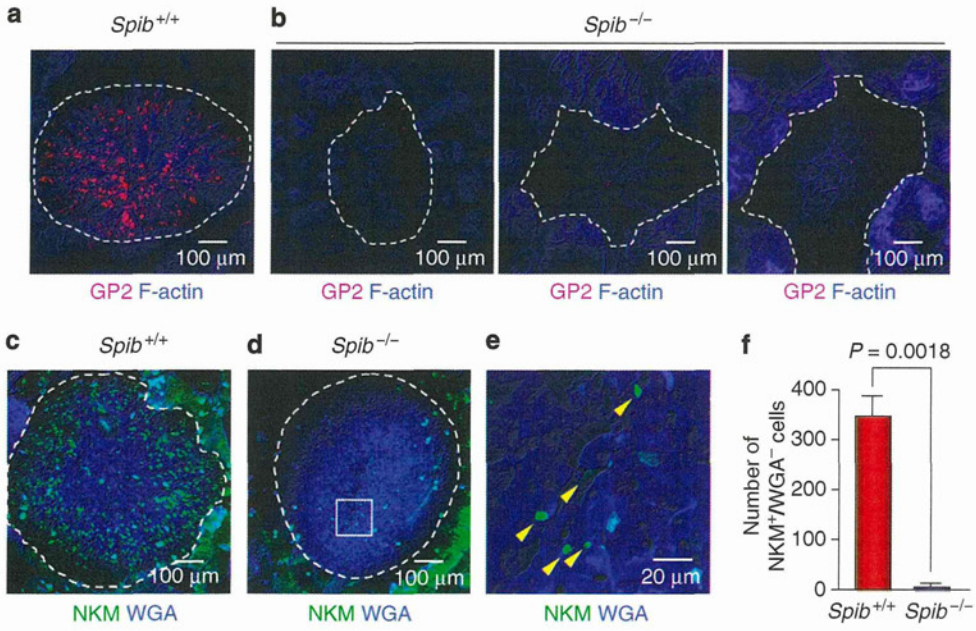

Figure 2 Abundance of surface markers on microfold cells (M cells) is severely diminished in Spi-B–deficient mice. Whole-mount staining analysis using anti-GP2 antibody (red; **a** and **b**) and NKM 16-2-4 antibody (green; **c**–**e**) in PPs from wild-type (**a** and **c**) and *Spib*$^{-/-}$ (**b** and **d**) mice. (**e**) High-magnification image of the white square in **d**. Data are representative of at least three independent experiments. (**f**) The number of NKM^{+} WGA^{-} cells found in one FAE region. Data are mean ± s.e.m. of one representative from three independent experiments. *P*-values were determined by Mann–Whitney *U*-test.

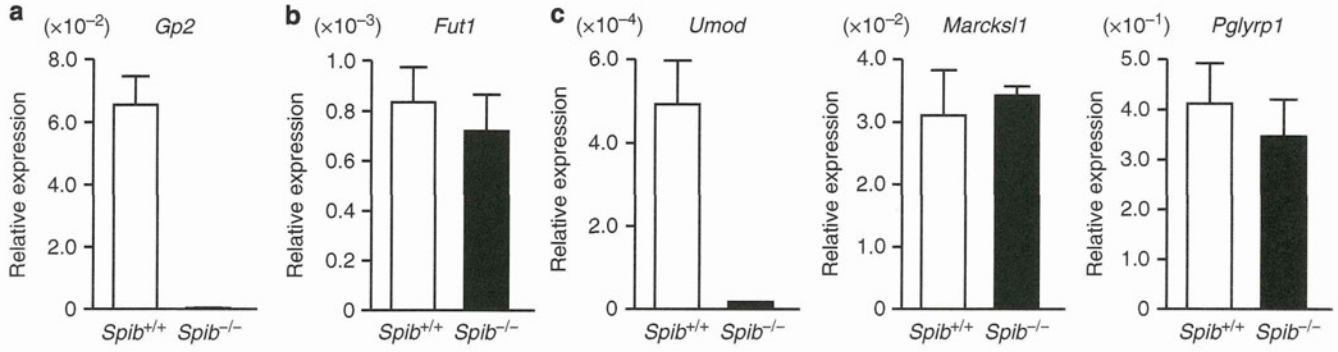

Figure 3 Spi-B–dependent and –independent expression of M-cell–specific genes. Real-time PCR analysis of the expression of several M-cell–specific genes (**a**, *Gp2*; **b**, *Fut1*; and **c**, *Umod*, *Marcksl1*, and *Pglyrp1*) in FAE prepared from *Spib*$^{+/+}$ and *Spib*$^{-/-}$ mice. Each result was normalized against the expression of *Gapdh* and is shown as the mean ± s.d. of one representative from three independent experiments. *P*-values were determined by Student's *t*-test.

enfolding lymphocytes was found in the *Spib*$^{-/-}$ M cells (**Supplementary Figure S2** online), as in the wild-type M cells.[13] These data are consistent with the whole-mount staining data we obtained with NKM/WGA, but not with anti-GP2 antibody (**Figure 2f,b**); they suggest that although the unique surface morphology of most M cells is also regulated by Spi-B, there is a small population of M cells (about 10 per FAE region; **Figure 2f**) of which differentiation is independent of Spi-B.

B-cell–intrinsic Spi-B is dispensable in the induction of M-cell–specific markers

Spib$^{-/-}$ mice showed a severe reduction in M-cell features, but Spi-B is expressed mainly in hematopoietic cells—particularly in B cells and plasmacytoid dendritic cells.[14–16] Moreover, one report has indicated that a certain B-cell subset residing in the subepithelial dome of the PP mucosa contributes to M-cell differentiation.[17] Therefore, we next investigated whether B cells (or T cells, or both) were responsible for the expression of GP2 on M cells. We used bone marrow (BM) chimeric mice, created by transplanting wild-type or *Spib*$^{-/-}$ BM cells into recombination activating protein 1 (RAG1)-deficient mice, which have no mature B and T lymphocytes.[18] The number of GP2^{+} cells in RAG1-deficient mice that received *Spib*$^{-/-}$ BM cells was comparable to the number in those that received wild-type BM cells (**Figure 5**), indicating that Spi-B expressed in B and T cells was not important in inducing or maintaining M-cell surface markers.

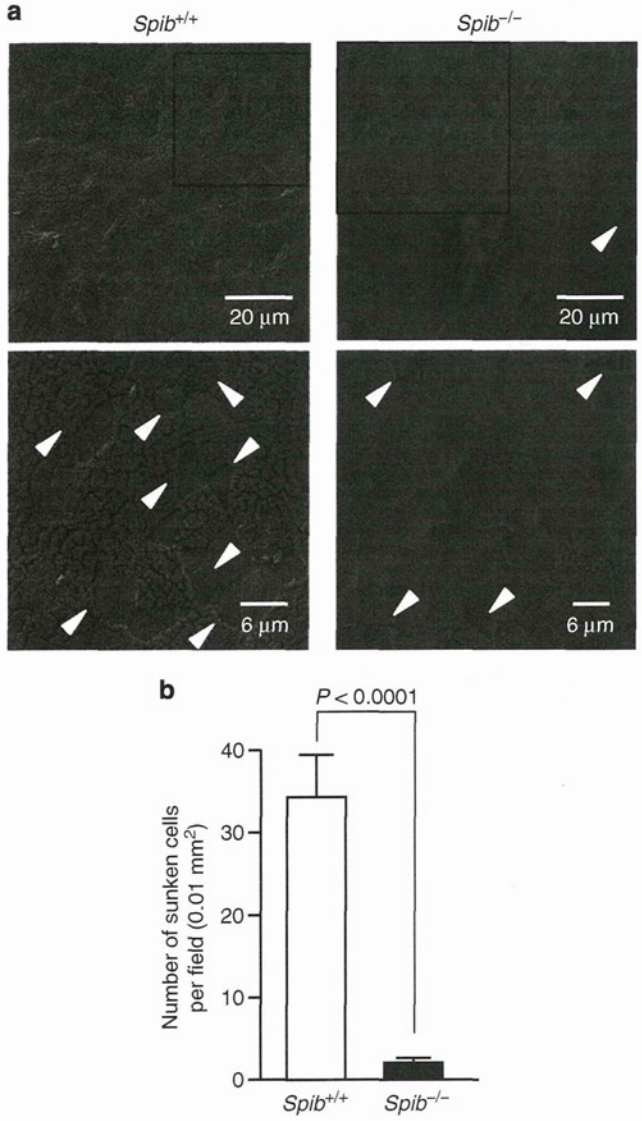

Figure 4 Number of sunken cells in FAE regions is decreased in Spi-B–deficient mice. (**a**) Scanning electron microscopic analysis of duodenal Payer's patch PPs from *Spib*$^{+/+}$ and *Spib*$^{-/-}$ mice. Typical M cells are indicated by arrowheads. Each bottom panel is a higher magnification of the box in each top panel. Data are representative of two independent experiments. (**b**) Calculated numbers of sunken cells per field. Data are means ± s.e.m. of one experiment representative of two independent experiments. *P*-values were determined by the Mann–Whitney *U*-test.

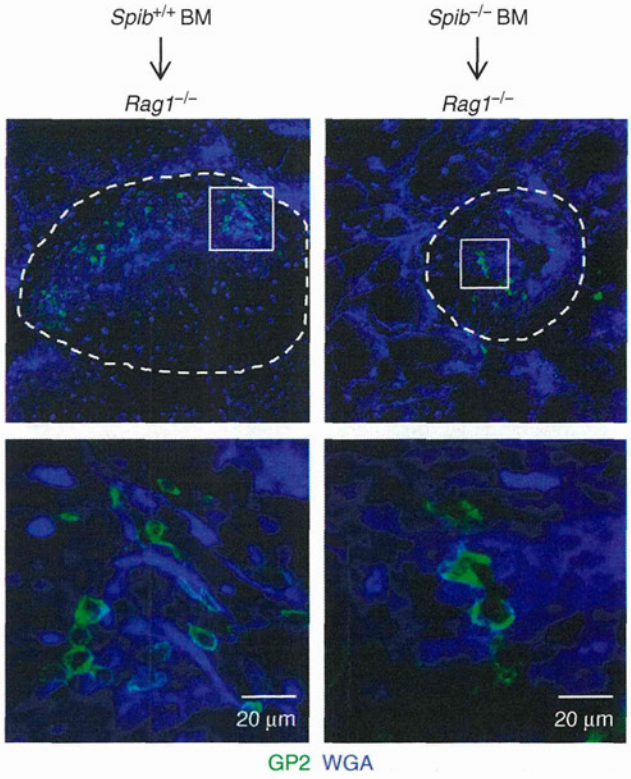

Figure 5 Spi-B expressed in B and T cells is not important for the expression of GP2 on M cells. Bone marrow (BM) cells were prepared from *Spib*$^{+/+}$ and *Spib*$^{-/-}$ mice and then transferred to RAG1-deficient mice. At 8 weeks after the transfer, GP2-positive FAE cells were visualized by whole-mount staining using anti-GP2 antibody (green). WGA was used for epithelial-cell counterstaining (blue). Each bottom panel is a higher magnification of the white square in each top panel. Data are representative of two independent experiments.

M cells differentiated by an Spi-B–independent pathway can transcytose PP-resident bacteria

M cells are specialized for antigen uptake.[1] Although small numbers of M cells were observed in the FAE region in *Spib*$^{-/-}$ mice (fewer than 5% of those in the wild type), it seemed that most M-cell features, such as expression of surface markers and apical morphology, were diminished in these mice. These findings raise the possibility that *Spib*$^{-/-}$ mice have diminished uptake of pathogenic or opportunistic bacteria, or both. Consistent with the loss of GP2 expression, uptake of *Salmonella* Typhimurium, which depends on host GP2 for binding to M cells, was markedly lower in *Spib*$^{-/-}$ mice than in wild-type mice (**Supplementary Figure S3** online).

We further examined whether PPs of *Spib*$^{-/-}$ mice possessed *Alcaligenes* spp., which, as we recently discovered, are opportunistic bacteria that inhabit inside PPs;[19] *Alcaligenes* spp. were moved from the lumen of the small intestine to the inside of the PPs preferentially via PP M cells (**Figure 6a**). Consistent with our previous reports,[19,20] *Alcaligenes* spp. had colonized the inside of the PPs well in wild-type mice (**Figure 6b**). Interestingly, intratissue *Alcaligenes* spp. were also detected inside the PPs from *Spib*$^{-/-}$ mice at levels almost comparable to those found in wild-type PPs (**Figure 6b**). Next, we examined *Alcaligenes* uptake capability in the PPs of *Spib*$^{-/-}$ mice by ligated-intestinal loop assay using culturable *A. faecalis*. Although *Spib*$^{-/-}$ mice showed a tendency toward reduced uptake, there was no significant difference between *Spib*$^{+/+}$ and *Spib*$^{-/-}$ mice in the translocation of *Alcaligenes* to the inside of the PPs (**Figure 6c**). These data indicated that *Alcaligenes* spp. could move to, and inhabit, the inside of the PPs, even if the host lacked Spi-B–dependent M cells.

DISCUSSION

In this study, we identified the novel M-cell–specific expression genes *Umod* and *Spib*. Spi-B-deficient mice showed complete

loss of GP2-positive M cells. However, these mice possessed small numbers of M cells, as defined by their pattern of reactivity to NKM/WGA and the ultrastructure of the apical surface, indicating that there are at least two nonredundant pathways for the development of PP M cells. Interestingly, although Spi-B regulated many other M-cell–specific genes, such as *Gp2*, expression of *Fut1*, *Marcksl1*, and *Pglyrp1* on M cells was observed to be independent of Spi-B (**Figure 3**). GP2 acts as a scaffold protein on M cells to transcytose FimH-positive type-I–piliated bacteria such as *S.* Typhimurium and *Escherichia coli*.[3] Therefore, GP2- and Spi-B–deficient mice showed low levels of uptake of these strains via M cells (Hase *et al.*[3] and **Supplementary Figure S3** online). Given that *Gp2* expression is under the control of Spi-B transcriptional activity, Spi-B has a critical role in M cells in regulating the uptake of FimH-positive bacteria.

Interestingly, although the expression of *Fut1* was independent of Spi-B, terminal fucosylation of PP M cells was severely diminished in *Spib*$^{-/-}$ mice. *Fut1* is specific to M cells among intestinal ECs, and terminal fucosylation on M cells is catalyzed by FUT1 (Terahara *et al.*[5] and **Supplementary Figure S1** online). Therefore, one possible explanation for our contradictory finding is that the expression of some molecules that are specifically expressed on M cells and are fucosylated by FUT1 is regulated by Spi-B. If a substrate for the fucosylation mediated by FUT1 was absent, M cells would not be detectable by NKM antibody and UEA-1. GP2 is a candidate for such a molecule, but both NKM antibody and UEA-1 react well with the M cells of GP2-deficient mice (**Supplementary Figure S4** online). The explanation presented above is compatible with our data in which M cells differentiated independently of Spi-B were fucosylated but did not express GP2 on their apical surfaces. Therefore, it may be of interest to look for differences in the FUT1-positive cells of wild-type and *Spib*$^{-/-}$ mice.

Several lines of evidence have indicated that non-intestinal ECs are involved in M-cell development. These cells include CCR6^{hi}CD11c^{int} B cells and RANKL-positive stromal cells, both of which are located in the subepithelial dome region under the FAE.[17,21] Although Spi-B is expressed mainly in lymphoid cells,[14,15] our results have shown that Spi-B is also expressed, and regulates the expression of some genes, in non-hematopoietic cells. In addition, our finding that *Spib*$^{-/-}$ B cells were sufficient for the induction or maintenance of M-cell surface markers showed that M-cell–, but not

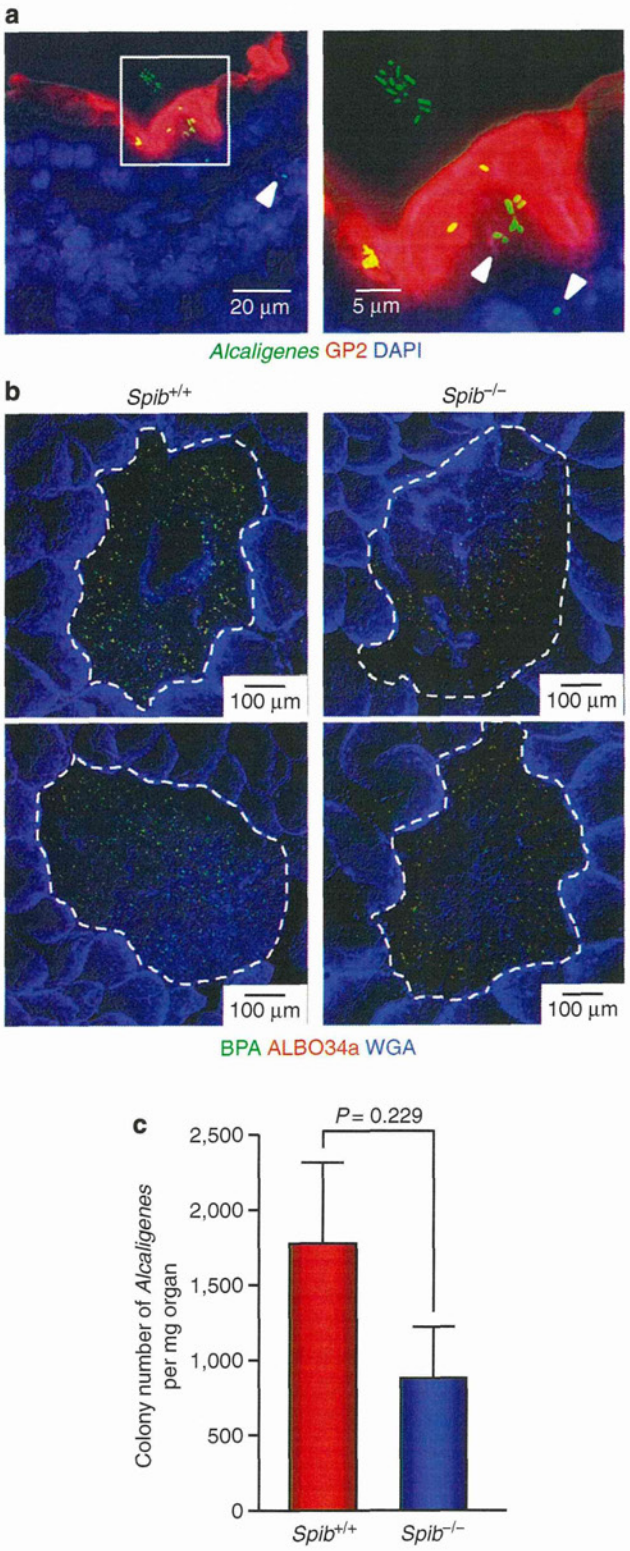

Figure 6 PP-resident commensal bacteria cohabit, and translocate within, the PPs preferentially through M cells. (**a**) GFP-expressed *Alcaligenes faecalis* were injected into ligated intestinal loops included in PPs. At 4 h after the injection, mice were euthanized and the PPs were dissected out. Fixed samples were sectioned and then stained with anti-GP2 antibody (red) and counterstained with 4′,6-diamidino-2-phenylindole (DAPI) (blue). M cells (GP2$^+$ cells) and GFP$^+$ *Alcaligenes* (green) were visualized under a fluorescence microscope (BZ-9000; Keyence). Transcytosed *Alcaligenes* are indicated by arrowheads. Data are representative of two independent experiments. (**b**) PPs from *Spib*$^{+/+}$ and *Spib*$^{-/-}$ mice were analyzed by fluorescent *in situ* hybridization (FISH) using probes to identify *Alcaligenes* spp. as BPA (green) and ALBO34a (red) doubly positive yellow dots. WGA was used for epithelial-cell counterstaining (blue). Data are representative of three independent experiments. (**c**) Uptake of culturable *Alcaligenes* on ligated-intestinal loop assay was quantified by counting colony numbers on streptomycin-containing culture plates. Results were normalized against PP weight, and data are means ± s.e.m. of one experiment representative of two independent experiments. *P*-values were determined by the Mann–Whitney *U*-test.

B-cell–, intrinsic Spi-B contributed to the development of M cells. Furthermore, the levels of RANKL expression in the PPs were similar in wild-type and *Spib*$^{-/-}$ mice (**Supplementary Figure S5** online). Taken together, these data indicate that M-cell–intrinsic Spi-B has a critical role in the functional development of Spi-B–dependent M cells.

Alcaligenes spp. are Gram-negative bacteria that reside within the PPs of not only mice but also humans and nonhuman primates.[19] Although we could not exclude the possibility that M-cell–independent uptake of *Alcaligenes* spp. occurred, our findings suggest that *Alcaligenes* spp. are preferentially transcytosed by M cells into the PPs (**Figure 6a**). The *Alcaligenes* spp. are then contained within the PPs by interleukin-22–producing innate lymphoid cells.[20] Although it is still not known whether *Alcaligenes* spp. are habituated to this environment and undergo a growth cycle there, or whether they are continuously supplied from outside, we observed this bacterial strain in the PPs of *Spib*$^{-/-}$ mice at levels comparable to those in the PPs of wild-type mice (**Figure 6b**). Given that *Spib*$^{-/-}$ mice possess fewer than 5% of the M cells of the wild-type, the few M cells that are present might be enough for the translocation and cohabitation of *Alcaligenes* spp. in the PPs. In fact, the M cells of *Spib*$^{-/-}$ mice showed the capability for preferential transcytosis of *Alcaligenes* (**Supplementary Figure S6** online). Indeed, our *ex vivo* ligated-loop assay showed that there was no significant difference between wild-type mice and *Spib*$^{-/-}$ mice in terms of the level of *Alcaligenes* transcytosis into the PPs, although the level tended to be lower in the latter (**Figure 6c**). Even though most of the cells found in the FAE of *Spib*$^{-/-}$ mice did not have M-cell features, it remains to be determined whether the FUT1-positive cells within the *Spib*$^{-/-}$ FAE, which in our study were putative "M cells," had really lost their transcytosis activity. Again, it will be important to investigate and compare the transcytosis abilities of FUT1-positive cells within the FAEs of wild-type and *Spib*$^{-/-}$ mice.

We found that, in addition to *Spib*, *Umod* is an M-cell–specific gene. *Umod* encodes THP (also known as uromodulin), which is a GP2 homolog and is expressed on the apical membrane of tubular ECs in the kidney. Membrane-bound THP is digested by the activity of phospholipase D or protease and released into the urine.[22] Secreted THP competitively binds to type-I–fimbriated *E. coli*, which can bind and internalize to the urothelium via FimH and host mannosylated uroplakins Ia and Ib.[23] THP thus helps to accelerate bacterial clearance. This information, together with our findings, suggests that THP contributes to the uptake of FimH-positive bacteria by PP M cells, although the level of *Umod* expression was very low compared with that of *Gp2* (**Figure 3a,c**).

During the preparation of this manuscript, Kanaya *et al.*,[24] using another line of Spi-B–deficient mice, and de Lau *et al.*,[25] using a "minigut" system, reported results similar to our data on Spi-B–dependent M-cell differentiation. Although there was a discrepancy between the results of these two groups in terms of the dependence of the expression of Annexin V (an M-cell–specific gene) on Spi-B, both groups reported that PP M cells were differentiated by RANKL stimulation via the induction of Spi-B in the M cells. They also reported that PP M cells were completely lost in Spi-B–deficient mice. In contrast to the above two reports, our study demonstrates that there is a population of PP M cells of which the differentiation mechanism is independent of Spi-B. Spi-B–deficient mice still possessed cells morphologically considered to be PP M cells (**Figure 4** and **Supplementary Figure S2** online). In addition, although the precise mechanism for the translocation of *Alcaligenes* spp. into PPs, including the nature of the host recognition receptor, has not been elucidated, substantial cohabitation of this opportunistic bacterium within, as well as its uptake into, PPs was observed in Spi-B–deficient mice (**Figure 6b,c**). Kanaya *et al.*[26] found much lower uptake of not only *S.* Typhimurium but also *Yersinia enterocolitica* (the host binding receptor of which is β1-integrin[26]) in the PPs of *Spib*$^{-/-}$ mice than in the wild type. Although they did not mention the levels of expression of β1-integrin, the reduced translocation of *Y. enterocolitica* might have been caused by a reduction in β1-integrin expression on the apical surfaces of the cells in *Spib*$^{-/-}$ PPs. Therefore, the difference in Spi-B dependency between bacterial species might be due to differences in the pathogenicity of the bacteria. The de Lau group[25] also proposed that RANKL induces the expression of other regulator genes for sufficient M-cell differentiation, because forced expression of Spi-B, but not RANKL, in the minigut system did not induce GP2 expression. These data raise the interesting possibility that other RANKL-induced regulators are involved in Spi-B–independent M-cell differentiation.

In conclusion, we discovered novel M-cell–specific genes, one of which, *Spib*, is a candidate master transcription factor for M-cell functional and structural maturation. Although M-cell–intrinsic Spi-B regulated most M-cell–specific gene expression, future studies are required to clarify in detail the mechanisms by which individual Spi-B target molecules contribute to M-cell function and maturation. In addition, the mechanisms of Spi-B–independent M-cell development and their contribution to the antigen-uptake function of these cells need to be demonstrated in future.

METHODS

Mice. RAG1-deficient mice were purchased from Jackson Laboratories (Bar Harbor, ME). *Gp2*$^{-/-}$ and *Fut1*$^{lacZ/lacZ}$ mice were kindly provided by Dr Anson W. Lowe[27] and Dr Steven E. Domino,[28] respectively. Spi-B–targeted mice on a C57BL/6 background were kindly provided by Dr LeeAnn Garrett-Sinha, with permission from Dr M. Celeste Simon.[15] Heterozygous mice were crossed to obtain *Spib*$^{+/+}$ and *Spib*$^{-/-}$ mice. Littermates or age- and gender-matched *Spib*$^{+/+}$ and *Spib*$^{-/-}$ mice were used for all subsequent experiments. All animals were housed in specific pathogen–free conditions at the animal facility of the Institute of Medical Science, The University of Tokyo. All animal experiments were carried out with the approval of the Animal Research Committee of the Institute of Medical Science, The University of Tokyo (Tokyo, Japan).

Preparation of small intestinal epithelial fractions. Small intestinal ECs were isolated as described previously.[2] Briefly, PPs and PP-free small intestines were treated with 0.5 mM ethylenediaminetetraacetic acid in phosphate-buffered saline (PBS) for 20 min at 37°C. Dissociated cells were filtered through a 40-μm nylon mesh, centrifuged,

and resuspended with Dulbecco's modified Eagle's medium supplemented with 10% fetal calf serum. ECs from PPs were stained with 5 μg ml^{-1} fluorescein isothiocyanate-conjugated NKM 16-2-4 monoclonal antibody,[13] 6 μg ml^{-1} rhodamine-labeled UEA-1 (Vector Laboratories, Burlingame, CA), and 1 μg ml^{-1} APC-Cy7-conjugated antimouse CD45 monoclonal antibody (BD Biosciences, Oxford, UK) for 40 min before being reacted with 7-aminoactinomycin D (BD Biosciences) for 10 min at 4°C. The stained cells were sorted with a flow cytometer FACSAria II (BD Biosciences); NKM$^+$/UEA-1$^+$/CD45$^-$ cells and NKM$^-$/UEA-1$^-$/CD45$^-$ cells were sorted as PP M cells and PP non-M cells, respectively. Dead cells were excluded on the basis of their positive reactivity to 7-aminoactinomycin D. To prepare FAE sheets, PPs were washed well with PBS and then soaked in 25 mM ethylenediaminetetraacetic acid in PBS for 15 min at room temperature. The FAE was peeled off by manipulation with fine needles under a stereoscopic microscope.

Real-time PCR. Total RNA was isolated from the cells by using an RNeasy Kit (Qiagen, Tokyo, Japan). Reverse transcription was performed with SuperScript VILO (Invitrogen, Carlsbad, CA). For quantitative PCR, cDNA products were amplified with a set of specific primers and LightCycler 480 SYBR Green I Master (Roche, Indianapolis, IN) on a LightCycler 480 System II (Roche). The mRNA expression level of each target was normalized against that of *Gapdh*. The sets of primers used were as follows: *Gapdh* (forward) 5′-TGTC CGTCGTGGATCTGAC-3′ and (reverse) 5′-CCTGCTTCACCAC CTTCTTG-3′; *Spib* (forward) 5′-GCCCACACTTAAGCTGTT TGTA-3′ and (reverse) 5′-CTGTCCAGCCCCATGTAGAG-3′; *Umod* (forward) 5′-GGATGGGGATCCCTTTGA-3′ and (reverse) 5′-GGCA TTCAGAACACCGTCTC-3′; *Gp2* (forward) 5′-GTGGGTTGTGA CCTGCTGT-3′ and (reverse) 5′-CTGGGCCTCCCATAACCT-3′; *Fut1* (forward) 5′-AAAGAATTCGCTTGCACCAC-3′ and (reverse) 5′-GAGAGCACACAGACCAACAGA-3′; *Marcksl1* (forward) 5′-GGC AGCCAGAGCTCTAAGG-3 and (reverse) 5′-TCACGTGGCCAT TCTCCT-3′; and *Pglyrp1* (forward) 5′-CAGTTCGCTACGTGGT GATCT-3′ and (reverse) 5′-TCTCCAATAAGGAAGTTGTAGG CTAC-3′.

***In situ* hybridization.** The DNA fragment encoding Spi-B (GenBank: NM_019866) or THP (GenBank: NM_009470) was amplified by PCR from BALB/c mouse embryo (14.5-day)–derived cDNA. The following primers were used: *Spib* (forward) 5′-CTCTGAACCACCATGC TTGCTCTGGAG-3′ and (reverse) 5′-GTACGGAGCATAAGCCA AGGAGCCCAG-3′; and *Umod* (forward) 5′-GTACCTAACCCATC CTTGCCTTTGGGC-3′ and (reverse) 5′-TCACAGGAGTAGCCCC ACACCATACTC-3′. The PCR products were subcloned into a pCR4-TOPO vector (Invitrogen). After the sequencing, digoxigenin-labeled sense and antisense RNA probes were transcribed *in vitro* with a digoxigenin RNA labeling mix (Roche). Paraffin-embedded sections of duodenal tissues (6 μm) from naïve BALB/c mice were obtained from Genostaff (Tokyo, Japan). The sections were fixed with 4% paraformaldehyde in PBS, and then treated with 20 μg ml^{-1} proteinase K in PBS for 30 min at 37°C. Hybridization was performed with 300 ng ml^{-1} probes at 60°C for 16 h. After hybridization, the bound probes were treated with anti-digoxigenin–AP conjugate (Roche) and visualized with NBT/BCIP solution (Sigma, St Louis, MO). After *in situ* hybridization, sections were counterstained with Kernechtrot stain solution (Muto Pure Chemicals, Tokyo, Japan) or reacted with 0.25 μg ml^{-1} biotin-conjugated UEA-1 after treatment with 0.3% H_2O_2. The sections were further reacted with HRP-conjugated streptavidin and then stained with diaminobenzidine (Vector Laboratories).

Whole-mount staining. PPs were excised from the duodenum and ileum and then washed with PBS. Isolated tissues were fixed and permeabilized with a Cytofix/Cytoperm kit (BD Biosciences) for GP2 staining, or just fixed with 4% paraformaldehyde for staining with NKM antibody. Specimens were then stained with anti-mouse GP2 antibody (MBL, Nagoya, Japan) or NKM 16-2-4 monoclonal antibody,[13] followed by secondary antibodies conjugated with Alexa Fluor 488 or Cy3 (Jackson ImmunoResearch, West Grove, PA). After being washed with PBS, the whole-mount specimens were further stained with Alexa Fluor 633-conjugated phalloidin (Invitrogen) or WGA (Invitrogen). All samples were mounted and then analyzed by DM IRE2/TCS SP2 confocal microscopy (Leica, Wetzlar, Germany).

To detect *Alcaligenes* spp., whole-mount fluorescent *in situ* hybridization analysis was performed as described previously.[19] X-gal staining to visualize FUT1 expression in tissues from *Fut1*$^{lacZ/+}$ mice was performed with a β-gal staining kit (Invitrogen) in accordance with the manufacturer's instructions.

Electron microscopy. PPs were fixed for 3 h at room temperature in a solution containing 2.5% glutaraldehyde, 2% paraformaldehyde, and 0.1 M of phosphate buffer (pH 7.5). After washes with 3% sucrose in 0.1 M of phosphate buffer, the tissues were fixed with 1% osmium tetraoxide on ice for 2 h and dehydrated with an ethanol series. For scanning electron microscopy, dehydrated samples were freeze-embedded in *t*-butyl alcohol and freeze dried, and then coated with osmium and observed under a scanning electron microscope (S-4200; Hitachi, Tokyo, Japan). For transmission electron microscopy, dehydrated samples were embedded in Epon 812 resin mixture (TAAB Laboratories, Aldermaston, UK) after treatment with propylene oxide. Ultrathin sections (90 nm) were stained with 2% uranyl acetate and Reynolds lead and examined under a Hitachi H-7500 electron microscope.

BM transfer. BM cells were prepared from *Spib*$^{+/+}$ and *Spib*$^{-/-}$ mice. The cells were intravenously injected into RAG1-deficient mice. The mice were analyzed 8 weeks after reconstitution.

Ligated-intestinal loop assay. Mice were anesthetized by using an isoflurane vaporizer. An intestinal loop containing a single PP was ligated off, and the lumen was then injected with 1×10^8 CFU/0.1 ml of *Alcaligenes*, which had been transformed with streptomycin resistance genes.[19] After 4 h, the mice were euthanized and the PP was excised from the ligated intestine. Specimens were extensively washed with PBS and then used to make a series of frozen sections or whole-mount stain to examine the uptake of *Alcaligenes*. To perform the colony-forming unit assay, washed tissues were incubated in 100 μg ml^{-1} gentamycin solution at room temperature for 30 min. After being washed with sterile PBS, all tissues were weighed, homogenized, and diluted with sterile PBS. The homogenates were then plated on LB agar plates containing 50 μg ml^{-1} streptomycin.

Colony-forming unit assay after *S.* Typhimurium oral infection. *Spib*$^{+/+}$ and *Spib*$^{-/-}$ mice were fed 1×10^8 CFU/0.1 ml of *S.* Typhimurium carrying a nalidixic acid resistance gene (strain χ3306, kindly provided by Dr Hidenori Matsui[29]). After 24 h, PPs were collected from the ileum region, extensively washed with PBS, and then incubated in 100 μg ml^{-1} gentamycin solution at room temperature for 30 min. After being washed with sterile PBS, all tissues were weighed, homogenized, and diluted with sterile PBS. The homogenates were then plated on LB agar plates containing 25 μg ml^{-1} nalidixic acid.

Statistical analysis. Results were compared by using Student's *t*-test and the Mann–Whitney *U*-test for parametric and nonparametric data, respectively. Statistical significance was established at $P < 0.05$.

SUPPLEMENTARY MATERIAL is linked to the online version of the paper at http://www.nature.com/mi

ACKNOWLEDGEMENTS

We thank Lee-Ann Garret-Sinha (The State University of New York at Buffalo, Buffalo, NY) and M. Celeste Simon (University of Pennsylvania School of Medicine, Philadelphia, PA) for providing the *Spib*$^{-/-}$ mice, Anson W. Lowe (Stanford University, Palo Alto, CA) for providing the

Gp2$^{-/-}$ mice, and Steven E. Domino (University of Michigan, Ann Arbor, MI) for providing the *Fut1*$^{lacZ/lacZ}$ mice. We also thank Hidenori Matsui (Kitasato University, Tokyo, Japan) for the *S.* Typhimurium; Hiroshi Sagara (The University of Tokyo, Tokyo, Japan) for electron microscopy; and Yoshihito Minoda, Jun Yoshida, and Ai Yamashita for technical assistance. Our work is supported by grants from: the Ministry of Education, Culture, Sports, Science, and Technology of Japan (Grant-in-Aid for challenging Exploratory Research (23659199 to S.S.) and for Scientific Research S (23229004 to H.K.)); the Global Center of Excellence Program of the Center of Education and Research for Advanced Genome-based Medicine (to H.K.); and the Core Research for Evolutional Science and Technology Program of the Japan Science and Technology Agency (to H.K.).

DISCLOSURE

The authors declared no conflict of interest.

REFERENCES

1. Neutra, M.R., Mantis, N.J. & Kraehenbuhl, J.P. Collaboration of epithelial cells with organized mucosal lymphoid tissues. *Nat. Immunol.* **2**, 1004–1009 (2001).
2. Terahara, K. *et al.* Comprehensive gene expression profiling of Peyer's patch M cells, villous M-like cells, and intestinal epithelial cells. *J. Immunol.* **180**, 7840–7846 (2008).
3. Hase, K. *et al.* Uptake through glycoprotein 2 of FimH(+) bacteria by M cells initiates mucosal immune response. *Nature* **462**, 226–230 (2009).
4. Lo, D. *et al.* Peptidoglycan recognition protein expression in mouse Peyer's patch follicle associated epithelium suggests functional specialization. *Cell. Immunol.* **224**, 8–16 (2003).
5. Terahara, K. *et al.* Distinct fucosylation of M cells and epithelial cells by Fut1 and Fut2, respectively, in response to intestinal environmental stress. *Biochem. Biophys. Res. Commun.* **404**, 822–828 (2011).
6. Sato, T. *et al.* Single Lgr5 stem cells build crypt–villus structures *in vitro* without a mesenchymal niche. *Nature* **459**, 262–265 (2009).
7. Yang, Q., Bermingham, N.A., Finegold, M.J. & Zoghbi, H.Y. Requirement of Math1 for secretory cell lineage commitment in the mouse intestine. *Science* **294**, 2155–2158 (2001).
8. Bastide, P. *et al.* Sox9 regulates cell proliferation and is required for Paneth cell differentiation in the intestinal epithelium. *J. Cell Biol.* **178**, 635–648 (2007).
9. Jenny, M. *et al.* Neurogenin3 is differentially required for endocrine cell fate specification in the intestinal and gastric epithelium. *EMBO J.* **21**, 6338–6347 (2002).
10. Katz, J.P. *et al.* The zinc-finger transcription factor Klf4 is required for terminal differentiation of goblet cells in the colon. *Development* **129**, 2619–2628 (2002).
11. Mori-Akiyama, Y. *et al.* SOX9 is required for the differentiation of Paneth cells in the intestinal epithelium. *Gastroenterology* **133**, 539–546 (2007).
12. Jensen, J. *et al.* Control of endodermal endocrine development by Hes-1. *Nat. Genet.* **24**, 36–44 (2000).
13. Nochi, T. *et al.* A novel M cell-specific carbohydrate-targeted mucosal vaccine effectively induces antigen-specific immune responses. *J. Exp. Med.* **204**, 2789–2796 (2007).
14. Schotte, R., Nagasawa, M., Weijer, K., Spits, H. & Blom, B. The ETS transcription factor Spi-B is required for human plasmacytoid dendritic cell development. *J. Exp. Med.* **200**, 1503–1509 (2004).
15. Su, G.H. *et al.* Defective B cell receptor-mediated responses in mice lacking the Ets protein, Spi-B. *EMBO J* **16**, 7118–7129 (1997).
16. Cisse, B. *et al.* Transcription factor E2-2 is an essential and specific regulator of plasmacytoid dendritic cell development. *Cell* **135**, 37–48 (2008).
17. Ebisawa, M. *et al.* CCR6hiCD11c(int) B cells promote M-cell differentiation in Peyer's patch. *Int. Immunol.* **23**, 261–269 (2011).
18. Mombaerts, P., Iacomini, J., Johnson, R.S., Herrup, K., Tonegawa, S. & Papaioannou, V.E. RAG-1-deficient mice have no mature B and T lymphocytes. *Cell* **68**, 869–877 (1992).
19. Obata, T. *et al.* Indigenous opportunistic bacteria inhabit mammalian gut-associated lymphoid tissues and share a mucosal antibody-mediated symbiosis. *Proc. Natl. Acad. Sci. USA* **107**, 7419–7424 (2010).
20. Sonnenberg, G.F. *et al.* Innate lymphoid cells promote anatomical containment of lymphoid-resident commensal bacteria. *Science* **336**, 1321–1325 (2012).
21. Knoop, K.A. *et al.* RANKL is necessary and sufficient to initiate development of antigen-sampling M cells in the intestinal epithelium. *J. Immunol.* **183**, 5738–5747 (2009).
22. Fukuoka, S., Freedman, S.D., Yu, H., Sukhatme, V.P. & Scheele, G.A. GP-2/THP gene family encodes self-binding glycosylphosphatidylinositol-anchored proteins in apical secretory compartments of pancreas and kidney. *Proc. Natl. Acad. Sci. USA* **89**, 1189–1193 (1992).
23. Pak, J., Pu, Y., Zhang, Z.T., Hasty, D.L. & Wu, X.R. Tamm–Horsfall protein binds to type 1 fimbriated *Escherichia coli* and prevents *E. coli* from binding to uroplakin Ia and Ib receptors. *J. Biol. Chem.* **276**, 9924–9930 (2001).
24. Kanaya, T. *et al.* The Ets transcription factor Spi-B is essential for the differentiation of intestinal microfold cells. *Nat. Immunol.* **13**, 729–736 (2012).
25. de Lau, W. *et al.* Peyer's patch M cells derived from Lgr5+ stem cells require SpiB and are induced by RankL in cultured "Miniguts". *Mol. Cell. Biol.* **32**, 3639–3647 (2012).
26. Vazquez-Torres, A. & Fang, F.C. Cellular routes of invasion by enteropathogens. *Curr. Opin. Microbiol.* **3**, 54–59 (2000).
27. Yu, S., Michie, S.A. & Lowe, A.W. Absence of the major zymogen granule membrane protein, GP2, does not affect pancreatic morphology or secretion. *J. Biol. Chem.* **279**, 50274–50279 (2004).
28. Domino, S.E., Zhang, L., Gillespie, P.J., Saunders, T.L. & Lowe, J.B. Deficiency of reproductive tract alpha(1,2)fucosylated glycans and normal fertility in mice with targeted deletions of the FUT1 or FUT2 alpha(1,2)-fucosyltransferase locus. *Mol. Cell. Biol.* **21**, 8336–8345 (2001).
29. Gulig, P.A., Doyle, T.J., Hughes, J.A. & Matsui., H. Analysis of host cells associated with the Spv-mediated increased intracellular growth rate of *Salmonella typhimurium* in mice. *Infect. Immun.* **66**, 2471–2485 (1998).

nature COMMUNICATIONS

OPEN

ARTICLE

Received 12 Apr 2012 | Accepted 27 Jul 2012 | Published 4 Sep 2012

DOI: 10.1038/ncomms2023

Extracellular ATP mediates mast cell-dependent intestinal inflammation through P2X7 purinoceptors

Yosuke Kurashima[1,2,3], Takeaki Amiya[1,3,4], Tomonori Nochi[1], Kumiko Fujisawa[1,3], Takeshi Haraguchi[5], Hideo Iba[5], Hiroko Tsutsui[6], Shintaro Sato[1,3], Sachiko Nakajima[7], Hideki Iijima[7], Masato Kubo[8,9], Jun Kunisawa[1,4] & Hiroshi Kiyono[1,2,3,4]

Mast cells are known effector cells in allergic and inflammatory diseases, but their precise roles in intestinal inflammation remain unknown. Here we show that activation of mast cells in intestinal inflammation is mediated by ATP-reactive P2X7 purinoceptors. We find an increase in the numbers of mast cells expressing P2X7 purinoceptors in the colons of mice with colitis and of patients with Crohn's disease. Treatment of mice with a P2X7 purinoceptor-specific antibody inhibits mast cell activation and subsequent intestinal inflammation. Similarly, intestinal inflammation is ameliorated in mast cell-deficient $Kit^{W\text{-}sh/W\text{-}sh}$ mice, and reconstitution with wild-type, but not $P2x7^{-/-}$ mast cells results in susceptibility to inflammation. ATP-P2X7 purinoceptor-mediated activation of mast cells not only induces inflammatory cytokines, but also chemokines and leukotrienes, to recruit neutrophils and subsequently exacerbate intestinal inflammation. These findings reveal the role of P2X7 purinoceptor-mediated mast cell activation in both the initiation and exacerbation of intestinal inflammation.

[1] Division of Mucosal Immunology, Department of Microbiology and Immunology, The Institute of Medical Science, The University of Tokyo, 108-8639, Japan. [2] Graduate School of Medicine, The University of Tokyo, 113-0033, Japan. [3] Core Research for Evolutional Science and Technology (CREST), Japan Science and Technology Agency (JST), Tokyo 102-0075, Japan. [4] Department of Medical Genome Science, Graduate School of Frontier Science, The University of Tokyo, Chiba 277-8561, Japan. [5] Division of Host-Parasite Interaction, Department of Microbiology and Immunology, The Institute of Medical Science, The University of Tokyo, 108-8639, Japan. [6] Department of Microbiology, Hyogo College of Medicine, Nishinomiya 663-8501, Japan. [7] Department of Gastroenterology and Hepatology, Osaka University Graduate School of Medicine, 565-0871, Japan. [8] Research Center for Allergy and Immunology, RIKEN, Yokohama Institute, Tsurumi, Yokohama, Kanagawa, 230-0045, Japan. [9] Division of Molecular Pathology, Research Institute for Biological Sciences, Tokyo University of Sciences, Chiba 278-0022, Japan. Correspondence and requests for materials should be addressed to J.K. (email: kunisawa@ims.u-tokyo.ac.jp) or to H.K. (email: kiyono@ims.u-tokyo.ac.jp).

Both active and quiescent immunity occur simultaneously to achieve immunological homoeostasis in the harshest of environments—namely, the intestine. Aberrant immune responses in the gut lead to the development of intestinal immune diseases such as colitis and food allergies[1,2]. Mast cells (MCs) are generally recognized as major effector cells of type 1 allergic diseases, as well as of inflammation, host defenses, innate and adaptive immune responses and homoeostatic responses[3–5]. Histological analyses of patients with, and murine models of, colitis have implicated the involvement of MCs in intestinal inflammation[4,6], but the factors responsible for MC activation are not fully understood.

Several lines of evidence have demonstrated that release of extracellular ATP and ADP from injured, dying or activated cells acts as a danger signal by modulating various cellular functions via the activation of P2 purinoceptors[7,8]. P2 purinoceptors comprise P2X ($P2X_{1-7}$) and P2Y receptors ($P2Y_{1, 2, 4, 6, 11-14}$). $P2X_{1-7}$ receptors are ATP-gated ion channels and specific for ATP, whereas P2Y receptors are G protein-coupled receptors that are specific for ADP, UTP and ATP[7,8].

Stimulation by ATP or ADP through the P2 purinoceptors of macrophages and dendritic cells (DCs) results in the production of inflammatory cytokines; this can lead to the development of asthma, contact hypersensitivity or graft-versus-host disease[9–11]. MCs also express several P2 purinoceptors and release histamine, cytokines and chemokines upon nucleotide stimulation[12]. Although MCs are thought to be involved in intestinal inflammation, it is unclear whether extracellular nucleotides are required for this process.

Here, we used a newly established anti-MC monoclonal antibody (mAb) to identify activated MCs and found that extracellular ATP mediates MC activation through P2X7 purinoceptors to initiate and amplify intestinal inflammation. Consequently, obstruction of the ATP-P2X7 purinoceptor cascade could be used to inhibit gut inflammatory diseases.

Results

Activated MCs in intestinal inflammation. Using a 2,4,6-trinitrobenzene sulphonic acid (TNBS)-induced colitis model, we first examined whether MCs were involved in intestinal inflammation. To assess MC activation *in vivo*, we established an mAb (clone: 5A9) specific for CD63, a marker of activated MCs[13]. We confirmed that our anti-CD63 mAb was reactive specifically to MCs activated by immunoglobulin (Ig)E plus relevant allergen or a calcium ionophore, and not to naïve and CD63-knocked down MCs (Supplementary Fig. S1). In the colons of TNBS-treated mice, increased numbers of $CD63^+$-activated MCs were noted until day 3 post administration; the numbers then gradually decreased and reached a basal level on day 6 (Fig. 1a,b), indicating that MC activation was associated with the initiation phase of colitis development, as previously reported in a murine model and in patients with inflammatory bowel disease[6,14]. It has generally been accepted that the mechanistic basis of ulcerative colitis (UC) and Crohn's disease (CD) are different. Indeed, the pathogenic cytokines involved in the development of UC and CD are different[2] and the genetic polymorphisms specific for UC and CD are also different[15]. In addition, the cytokines required for the development of MCs differ between humans (stem cell factor) and mice [interleukin (IL)-3 and stem cell factor][4]. Thus, these different pathological environments may have led to differences in the requirement for, and involvement of, MCs in the development of inflammation. Therefore, we analysed MC numbers in both UD and CD patients, although we focused on the TNBS-induced colonic inflammation model. We detected increased numbers of MCs in the colons of patients with CD or UC (Fig. 1c,d). Thus, increased numbers of MCs in the colon is a characteristic of intestinal inflammation.

To directly show the involvement of MCs in the development of intestinal inflammation, we used MC-deficient $Kit^{W\text{-}sh/W\text{-}sh}$ mice. We confirmed that immunological and inflammatory symptoms induced by TNBS treatment were identical in $Kit^{W\text{-}sh/+}$ heterozygous and $Kit^{+/+}$ homozygous mice; however, inflammatory symptoms, such as body weight loss, massive inflammatory cell infiltration and colon shortening, were restored in $Kit^{W\text{-}sh/W\text{-}sh}$ mice but not in $Kit^{W\text{-}sh/+}$ heterozygous and $Kit^{+/+}$ homozygous mice (Fig. 1e–h). Similarly, our histological and immunological analyses revealed that destruction of the colonic epithelial layer and infiltration by inflammatory cells—especially neutrophils, which were stained neutral pink and had lobulated nuclei,—were reduced in $Kit^{W\text{-}sh/W\text{-}sh}$ mice (Fig. 1f,h,i). Moreover, inflammatory signs were ameliorated in $Kit^{W\text{-}sh/W\text{-}sh}$ mice when we used other well-known inflammatory bowel disease models, such as the dextran sodium sulphate (DSS) colitis model (Fig. 2a–c). As the use of $Kit^{W\text{-}sh/W\text{-}sh}$ mice as an MC-deficient model is controversial[16,17], we also used the MC-specific enhancer-mediated toxin receptor-mediated conditional cell knockout (TRECK) system (Mas-TRECK mice)[18]. We confirmed that specific depletion of MCs ameliorated the inflammation in this DSS-induced colitis model (Fig. 2d–h). Our data indicate that activated MCs participate in the aggravation of intestinal inflammation.

Establishment of an inhibitory MC-specific mAb. IgE plus a relevant allergen induces MC activation; however, $Rag\text{-}1^{-/-}$ and $Tcr\beta^{-/-}\delta^{-/-}$ mice showed inflammatory responses comparable to those in TNBS-induced intestinal inflammation (Supplementary Fig. S2a–d)[19] and had increased numbers of $CD63^+$-activated MCs in their colons (Supplementary Fig. S2e), suggesting that T and B cells are not involved in MC activation during colitis. We also found no increase in CD63 expression on MCs after stimulation with IL-18 and IL-33, which are known to be involved in colitis (Supplementary Fig. S2f)[20,21].

We next tried to establish an anti-MC mAb that could ameliorate activated MC-mediated intestinal inflammation. We immunized rats with purified murine-activated colonic MCs, established hybridomas, performed flow cytometry to select hybridomas that produced mAbs that preferentially recognized colonic MCs and examined the hybridomas' ability to inhibit ovalbumin-induced food allergy[22] or TNBS-induced intestinal inflammation (Supplementary Fig. S3). Among 2,000 clones, we obtained an anti-MC mAb (designated clone 1F11; rat IgG2b) that was strongly reactive to colonic MCs (Fig. 3a; Supplementary Fig. S3). In addition to colonic MCs, 1F11 mAb bound efficiently to peritoneal cavity-, lung- and bone marrow (BM)-derived MCs, but not to skin MCs (Fig. 3a). When tested with other immunocompetent cells in the colon, 1F11 mAb was weakly reactive to some $CD3^+$ T cells, $CD11c^+$ DCs and $F4/80^+$ macrophages, but was not reactive to $Gr\text{-}1^+$ granulocytes, IgA^+ plasma cells or epithelial cells (ECs) (Fig. 3b).

To show the inhibitory function of 1F11 mAb in intestinal inflammation, mice were given 1F11 mAb ($0.5\,mg\,day^{-1}$ in a single dose) for 3 days, beginning 1 day before intrarectal administration of TNBS. 1F11 mAb treatment reduced the intestinal inflammation (Fig. 3c–g) and decreased the number of $CD63^+$-activated MCs in 1F11 mAb-treated mice (Fig. 3h).

Targeting P2X7 receptors reduces intestinal inflammation. Mass spectrometry analyses of immunoprecipitants of MC cell lysates with 1F11 mAb showed that the P2X7 purinoceptor is recognized by 1F11 mAb (Supplementary Fig. S4a). The specificity of 1F11 mAb for the P2X7 purinoceptor was confirmed by its specific reactivity to cells transfected with P2X7 receptors but not with other types of P2X receptor (for example, P2X1 and P2X4; Supplementary Fig. S4b). MCs derived from $P2x7^{-/-}$ mice, however, were not recognized by 1F11 mAb (Supplementary Fig. S4c). Western blot and flow cytometric analysis showed that, among the several variants of P2X7 purinoceptors[23], 1F11 mAb bound to variant a (full-length; Supplementary Fig. S4d,e). In contrast, variant c (possessing

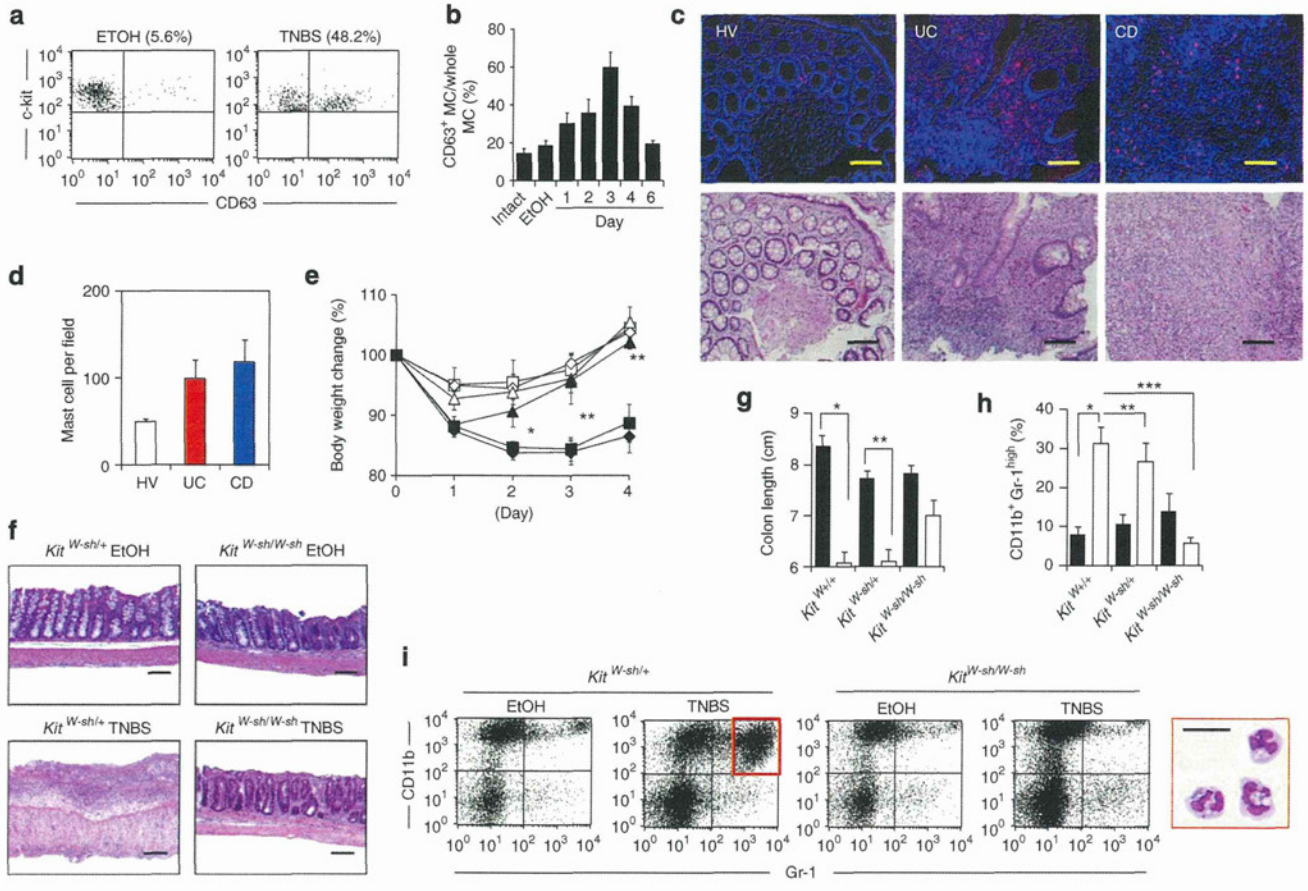

Figure 1 | Role of activated intestinal MCs in the development of intestinal inflammation. (**a**) CD63 expression on colonic MCs was examined with flow cytometry. Cells were gated on c-kit$^+$ and FcεRIα$^+$ cells. (**b**) The percentage of CD63$^+$ MCs in all c-kit$^+$ FcεRIα$^+$ MCs was determined with flow cytometry at various time points after TNBS administration ($n=3$ for day 6, $n=5$ for day 3, $n=7$ for intact, EtOH, day 1 and 2, $n=14$ for day 4). Control mice were analysed 4 days after EtOH administration (EtOH; $n=7$). Data are shown as means±s.e.m. (**c**) Colonic tissue sections from a healthy volunteer (HV) and UC and CD patients were stained with 4′,6-diamidino-2-phenyl indole (blue) and MC tryptase (red) or haematoxylin and eosin (H&E) (bottom). Scale bars, 100 μm. (**d**) Tryptase-positive MCs were counted in the fields of the tissue sections (four fields for each section). Data are means±s.e.m. ($n=6$). (**e**) Body weight changes were monitored after TNBS administration to *Kit* $^{W\text{-}sh/W\text{-}sh}$ MC-deficient mice (*Kit* $^{W\text{-}sh/W\text{-}sh}$ EtOH; open triangles: $n=4$, *Kit* $^{W\text{-}sh/W\text{-}sh}$ TNBS; closed triangles: $n=9$), *Kit* $^{+/+}$ control mice (*Kit* $^{+/+}$ EtOH; open diamonds: $n=4$, *Kit* $^{+/+}$ TNBS; closed diamonds: $n=13$) and *Kit* $^{W\text{-}sh/W+}$ control mice (*Kit* $^{W\text{-}sh/W+}$ EtOH; open squares: $n=4$, *Kit* $^{W\text{-}sh/W+}$ TNBS; closed squares: $n=11$). Data are shown as percentages of baseline weights and are means±s.e.m., $^*P<0.0001$ (two-tailed Student's *t*-test); $^{**}P=0.0024$ (two-tailed Student's *t*-test). (**f**) The colon was isolated 4 days after TNBS treatment for H&E staining. Data are representative of at least three independent experiments. Scale bars, 100 μm. (**g**) Colon length was measured 4 days after colitis induction. EtOH, closed column; TNBS, open column. $^*P<0.0001$ (two-tailed Student's *t*-test), $^{**}P=0.0024$ (two-tailed Student's *t*-test). Data are shown as means±s.e.m. (**h**) The percentage of CD11b$^+$ Gr-1^{high} cells in the colonic lamina propria was calculated, as measured with flow cytometry. EtOH, closed column; TNBS, open column. $^*P=0.0003$ (two-tailed Student's *t*-test), $^{**}P=0.0029$ (Welch's *t*-test) and $^{***}P<0.0001$ (Welch's *t*-test). Data are shown as means±s.e.m. (**i**) Colonic mononuclear cells were isolated 4 days after TNBS administration and stained with anti-CD11b and anti-Gr-1 antibodies. CD11b$^+$ Gr-1^{high} cells were sorted and then stained with May-Giemsa stain. Scale bar, 20 μm. Data are representative of three experiments.

the ATP-binding portion but lacking the C-terminal region) was detected by western blot, but its surface expression was not detected by flow cytometry because of its defect in extracellular expression (Supplementary Fig. S4d,e)[24]. In addition, neither western blot nor flow cytometry detected variant d (lacking the ATP-binding portion; Supplementary Fig. S4d,e). These data strongly suggest that 1F11 mAb recognizes P2X7 receptors, specifically the ATP-binding portion. We also confirmed that 1F11 mAb had similar reactivity to that of a commercially available anti-P2X7 mAb (clone: Hano43; Supplementary Fig. S4f,g).

To evaluate whether 1F11 mAb directly affects MCs during ATP-mediated activation, we treated MCs with ATP in the presence of 1F11 mAb *in vitro*. 1F11 mAb treatment reduced the number of CD63$^+$-activated MCs induced by ATP in a dose-dependent manner (Fig. 4a). High concentrations of extracellular ATP increased the cell permeability of the MCs[12]. Thus, uptake of Lucifer yellow was observed in ATP-stimulated MCs but was substantially impaired in 1F11 mAb-treated and *P2x7*$^{-/-}$ MCs (Fig. 4b,c).

As many cell types (MCs, T cells and DCs) express P2X7 receptors (Fig. 3b), we then asked whether the P2X7 receptors on MCs were responsible for the MC-mediated intestinal inflammation *in vivo* by analysing MC-deficient *Kit*$^{W\text{-}sh/W\text{-}sh}$ mice reconstituted with *P2x7*$^{+/+}$ or *P2x7*$^{-/-}$ MCs. We confirmed that reconstituted MCs were present in the colon and maintained P2X7 expression (Supplementary Fig. S5). Like wild-type mice, *Kit*$^{W\text{-}sh/W\text{-}sh}$ mice reconstituted with *P2x7*$^{+/+}$ MCs showed severe inflammatory responses when treated with TNBS. However, these inflammatory responses were ameliorated when *Kit*$^{W\text{-}sh/W\text{-}sh}$ mice were reconstituted with *P2x7*$^{-/-}$ MCs; the amelioration included inhibition of neutrophil infiltration and MC activation (Figs 1 and 5a–f).

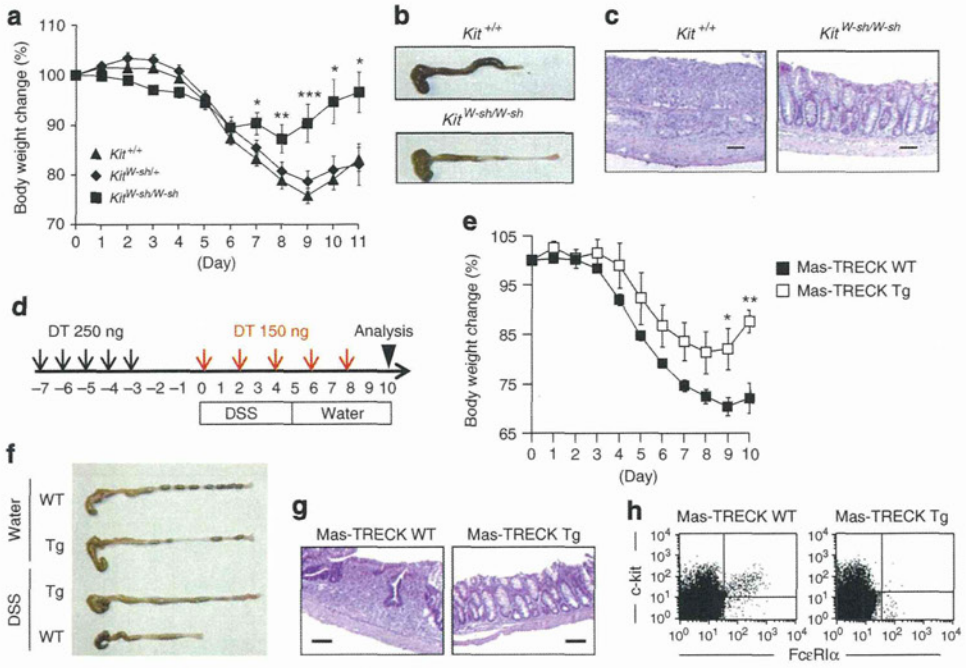

Figure 2 | Impaired DSS-induced colitis in MC-deficient mice. *Kit*$^{W\text{-}sh/W\text{-}sh}$ MC-deficient, *Kit*$^{+/+}$ control mice and Mas-TRECK transgenic (Tg) mice were subjected to DSS-induced colitis. (**a**) Body weight changes are shown as percentages of the baseline value and are means±s.e.m. ($n=22$ for *Kit*$^{+/+}$; $n=25$ for *Kit*$^{W\text{-}sh/+}$; $n=10$ for *Kit*$^{W\text{-}sh/W\text{-}sh}$). $^{*}P<0.01$, $^{**}P=0.0207$ and $^{***}P=0.0004$ (two-tailed Student's *t*-test). (**b**,**c**) Eleven days after DSS treatment, colon tissue and haematoxylin and eosin (H&E)-stained tissue sections were examined. Data are representative of at least three independent experiments. (**d**) Mas-TRECK Tg mice and their wild-type (WT) littermates were subjected to DSS-induced colitis. For diphtheria toxin (DT) treatment, mice were injected intraperitoneally with 250 ng of DT for 5 consecutive days (black arrows) and then with 150 ng every other day (red allows). (**e**) Body weight changes are shown as percentages of the baseline value and are means±s.e.m. ($n=6$ for Tg; $n=10$ for WT), $^{*}P=0.0107$, $^{**}P=0.0037$ (two-tailed Student's *t*-test). (**f**) Representative images of whole colons 10 days after DSS treatment. (**g**) Representative images of H&E staining. Scale bars, 100 μm. (**h**) Representative flow cytometric data of infiltrated c-kit^{+} FcεRIα^{+} MCs in the colon.

We next analysed whether the MCs in UC or CD patients expressed P2X7. Although increased number of MCs were observed in the colons of both UC and CD patients (Fig. 1c,d), P2X7 purinoceptors were expressed by the MCs in CD patients but not by those in UC patients or healthy volunteers (Fig. 5g,h). Thus, it is likely that P2X7 purinoceptor-mediated MC activation also occurs in the human colon, especially in CD patients.

To examine whether ATP was extracellularly released at high concentrations at inflammatory sites, we next measured ATP release from inflammatory colonic tissues. An elevated level of ATP release from the colon tissue was noted in TNBS-treated mice (Fig. 6a). In addition, intrarectal administration of non-hydrolyzable ATP (adenosine 5′-*O*-(3-thio) triphosphate and *O*-(4-benzoyl)benzoyl adenosine 5′-triphosphate) led to MC activation in the colonic tissue, similar to the effect of TNBS treatment (Fig. 6b). In contrast, intrarectal administration of other P2Y receptor agonists did not increase colonic MC activation (Fig. 6b). These findings indicate that inflammatory stimuli induce the extracellular release of ATP, which in turn leads to P2X7-dependent MC activation in the colon and subsequent exacerbation of intestinal inflammation.

P2X7 signalling activates the caspase-1 inflammasome to induce the production of IL-1β and IL-18 (ref. 25). IL-1β production is also mediated by MC proteases, such as chymases[26]. We therefore examined whether MCs produced IL-1β via P2X7 receptor activation, and if so whether this production was caspase-1-dependent. IL-1β production was decreased when P2X7-deficient MCs were stimulated with ATP, whereas substantial amounts of IL-1β were produced in caspase-1-deficient MCs (Supplementary Fig. S6), indicating that IL-1β production was P2X7-dependent but caspase-1-independent. In line with this finding, body weight changes were noted in *Kit*$^{W\text{-}sh/W\text{-}sh}$ mice reconstituted with *caspase-1*$^{-/-}$ MCs (Fig. 5a). These results suggest that MC-dependent inflammation through P2X7 purinoceptors is not dependent on caspase-1-mediated IL-1β or IL-18 production.

An autocrine loop of ATP conversion mediates MC activation. In addition to ATP, other nucleotides (for example, extracellular ADP) act as signals to induce inflammatory responses[27]. We confirmed that MCs are activated by high concentrations of ADP and ATP (Fig. 7a,b). Extracellular ATP is hydrolysed by ectonucleoside triphosphate diphosphohydrolases (CD39) to ADP and AMP; it is then further hydrolysed by ecto-5′-nucleotidase (CD73) to adenosine, which has anti-inflammatory functions[27]. Colonic MCs expressed CD39 but not CD73 (Supplementary Fig. S7a,b), indicating that MCs can convert ATP to ADP but not to adenosine. We therefore examined the involvement of ADP-reactive P2Y purinoceptors and found that P2Y1 and P2Y12 were highly expressed on colonic MCs (Fig. 7c). However, inhibitors of P2Y1 and P2Y12 receptors, as well as knockdown of the P2Y12 receptor, had no effect on the induction of CD63^{+}-activated MCs (Fig. 7d,e; Supplementary Fig. S8a). Similarly, intestinal inflammation, as well as activation of colonic MCs, was unaffected in clopidogrel (a P2Y12 receptor inhibitor)-treated mice (Supplementary Fig. S8b–d). These data indicate that although P2Y1 and P2Y12 were expressed on MCs neither P2Y1 nor P2Y12 purinoceptors mediate ADP-dependent CD63^{+} MC induction.

It is generally accepted that P2X7 purinoceptors specifically recognize ATP[7], but we found that they were also involved in ADP-mediated MC activation. Indeed, no activation was noted in *P2x7*$^{-/-}$ MCs when they were stimulated with ADP (Fig. 7f), leading us to hypothesize that ADP promotes ATP release from MCs and their subsequent stimulation. To test this hypothesis, we measured the expression of pannexin-1, connexin 43 and connexin 32, which

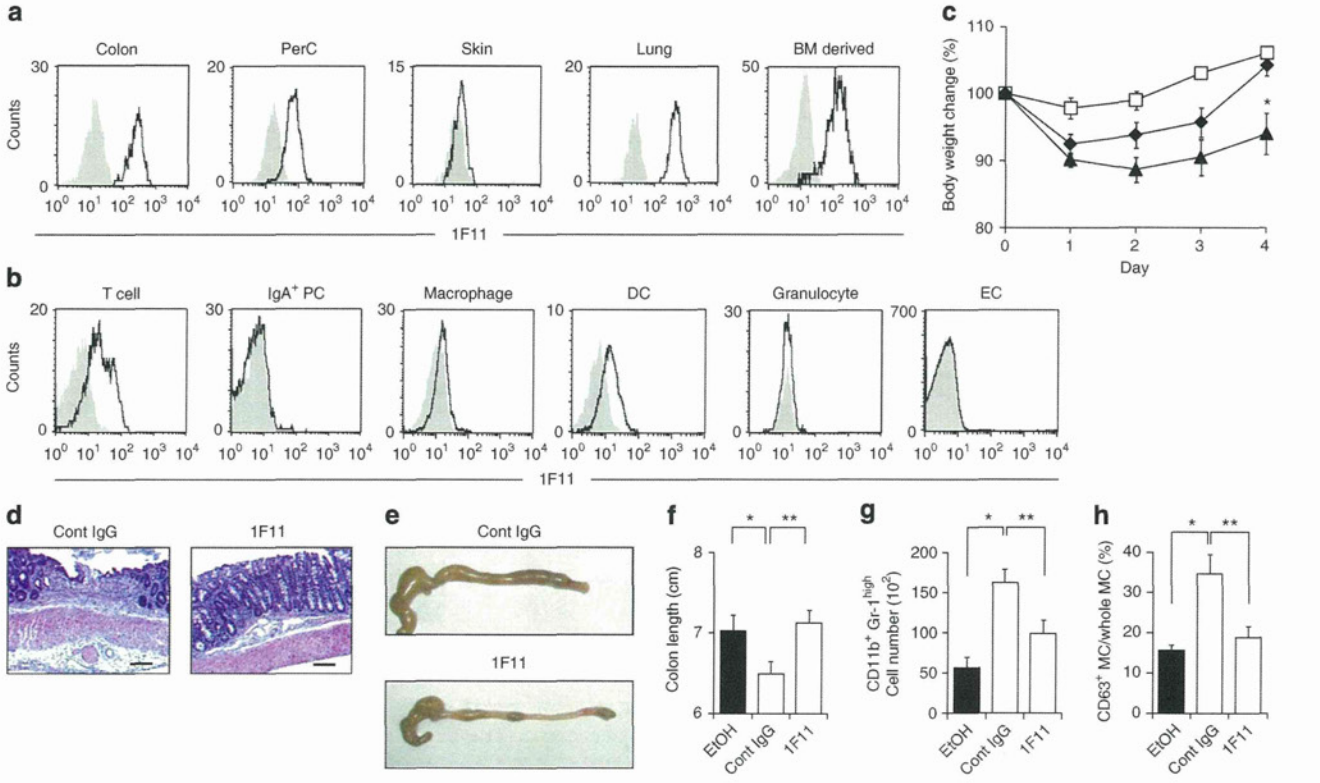

Figure 3 | Amelioration of colitis by treatment with intestinal MC-reactive 1F11 mAb. (**a**) MCs in the colonic lamina propria, peritoneal cavity (PerC), skin and lung, as well as BM-derived MCs, were stained with 1F11 mAb. Control staining with rat IgG2b is shown in grey. (**b**) Cells were isolated from colonic lamina propria and epithelium. CD3$^+$ T cells, IgA$^+$ plasma cells (PCs), F4/80$^+$ macrophages, CD11c$^+$ DCs, Gr1$^+$ granulocytes and ECs were gated and their reactivity to 1F11 mAb examined. Control staining with rat IgG2b is shown in grey. (**c**) C57BL/6 mice were treated with TNBS and their body weights were monitored for 4 days; 0.5 mg of 1F11 or the control mAb was intraperitoneally administered. Data from 9 (EtOH; open squares), 19 (TNBS with control mAb; closed triangles) and 12 (TNBS with 1F11 mAb; closed diamonds) mice. *P = 0.0066 (Welch's t-test). Data are shown as percentages of baseline weights and are means ± s.e.m. (**d**,**e**) Representative images of haematoxylin and eosin staining and colon tissue from 1F11 mAb-treated mice. Scale bars, 100 μm. (**f**) Colon length was measured 4 days after TNBS administration. *P = 0.0445; **P = 0.0073 (two-tailed Student's t-test). (**g**) Neutrophils (CD11b$^+$ Gr-1^{high}) were quantified as percentages and numbers of cells. Data are shown as means ± s.e.m. (n = 6), *P < 0.0001, **P = 0.0047 (two-tailed Student's t-test). (**h**) Percentage of CD63$^+$ MCs in all c-kit$^+$ FcεRIα$^+$ MCs was determined with flow cytometry. Data are shown as means ± s.e.m. (n = 6) *P = 0.0202; **P = 0.0284 (two-tailed Student's t-test).

are ATP-releasing hemichannels, during cell activation[28,29]. The hemichannels were rarely expressed on the colonic MCs (Fig. 7g), and no inhibitory effect was observed when the MCs were treated with ADP in the presence of hemichannel inhibitors (flufenamic acid and carbenoxolone). However, cell activation was inhibited by P2X7 antagonists [oxidized ATP (OxATP), pyridoxal-phosphate-6-azophenyl-2′,4′-disulfonate and 4,4′-diisothiocyanatostilbene-2,2′-disulfonic acid disodium salt hydrate] (Fig. 7h). To further exclude the possibility that ADP triggers ATP release, we stimulated MCs with another P2Y ligand (UTP); we found that UTP did not induce MC activation (Fig. 7b).

We then tested whether ADP was converted to ATP by ATP-converting enzymes such as ecto-adenylate kinase, ATP synthase and nucleoside diphosphokinase[30]. To test the involvement of these enzymes, we used inhibitors of ecto-adenylate kinase (diadenosine pentaphosphate; AD2P5), ATP synthase (oligomycin; oligo) and nucleoside diphosphokinase (UDP), and we found that inhibition of ecto-adenylate kinase and ATP synthase, but not nucleoside diphosphokinase, reduced ADP- as well as ATP-dependent MC activation (Fig. 7h,i). Neither AD2P5 nor oligo inhibited MC activation induced by the crosslinking of IgE with relevant allergen (Fig. 7i). Among the adenylate kinases, adenylate kinase 1 (AK1) and AK2 were expressed in colonic MCs, and the expression of AK2 was much higher than that of AK1 (Supplementary Fig. S9a). As with AD2P5 treatment, knockdown of AK2, but not AK1, led to the inhibition of both ADP- and ATP-mediated MC activation (Supplementary Fig. S9b). These results indicate that P2X7 purinoceptors have an important role in the activation of MCs by ATP, including ATP derived from ADP by the action of ecto-enzymes such as ATP synthase and AK2.

Neutrophil infiltration by MC-derived mediators. Evaluation of MC activation on the basis of CD63 expression is an important criterion[13]; however, degranulation is not absolutely associated with cytokine production[31]. Therefore, we measured MC production of an array of inflammatory cytokine, chemokine and lipid mediators to additionally elucidate the role of P2X7 purinoceptor-mediated MC activation in the development of intestinal inflammation. Stimulation of MCs with ATP induced the production of inflammatory cytokines such as IL-6, tumour necrosis factor (TNF)α and oncostatin M[32]; this induction was not observed in *P2x7*$^{-/-}$ MCs or in wild-type MCs treated with 1F11 mAb (Fig. 8a,b).

We showed that neutrophil infiltration into the colon was mediated by MC activation (Fig. 1h,i), and a previous study suggested that neutrophil infiltration is a potential target in colitis treatment[33]. Consistent with these findings, ATP stimulation induced MCs, but not *P2x7*$^{-/-}$ MCs, to produce leukotrienes (LTs; LT C4/D4/E4), which are associated with the translocation of 5-lipoxygenase (5-LO) into the nucleus—an important step for LT synthesis in MCs[34] (Fig. 8c,d). Also, chemokine gene array analysis demonstrated that